Drug Metab. Pharmacokinet. 19 (6): *SNP33* (453)–*SNP35* (455) (2004).

SNP Communication

A Novel Variant Allele of OATP-C (SLCO1B1) Found in a Japanese Patient with Pravastatin-induced Myopathy

Kaori MORIMOTO[1], Tomoharu OISHI[1], Shiro UEDA[2], Madoka UEDA[1], Masakiyo HOSOKAWA[1] and Kan CHIBA[1]

[1]*Laboratory of Pharmacology and Toxicology and* [2]*Department of Drug Information and Communication, Graduate School of Pharmaceutical Sciences, Chiba University, Chiba, Japan*

Full text of this paper is available at http://www.jssx.org

Summary: We have recently found that the frequency of *OATP-C*15* is significantly higher in patients who experienced myopathy after receiving pravastatin or atorvastatin than in patients without myopathy. However, there were two patients who experienced pravastatin-induced myopathy despite the fact that they did not possess *OATP-C*15* or other known mutations of *OATP-C* that have been reported to decrease the function of OATP-C. In this study, we sequenced all of the exons and exon-intron junctions of *OATP-C* of the two patients and found a novel mutation in exon 12 of *OATP-C* in one of the patients. In this mutation (1628T>G), there is a substitution of Leu to Trp at position 543 in transmembrane-spanning domain 10 of OATP-C. However, the frequency of this mutation in the Japanese population appears to be very low (<1%).

Key words: ***OATP-C (SLCO1B1)*; novel variant allele; nonsynonymous; statins**

Introduction

3-Hydroxy-3-methylglutaryl coenzyme A reductase inhibitors, also known as statins, are the most effective drugs for treatment of elevated concentration of low-density lipoprotein cholesterol, and they have been shown to reduce cardiovascular events of coronary heart disease and cardiovascular-related morbidity and mortality rates.[1] These drugs are tolerated well by most patients, but they can produce a variety of muscle-related complaints like myopathy and rhabdomyolysis, which have been the major clinical complication for statin treatment.[2] We have recently studied genetic factors contributing to the risk of statin-induced myopathy and found that the frequency of *OATP-C*15*, a mutant allele of *OATP-C* (OATP1B1, gene *SLC21A6/SLCO1B1*), was significantly higher in patients with myopathy who were receiving pravastatin or atorvastatin than in patients without myopathy.[3] We also found in another study that transporting activities for pravastatin and atorvastatin decreased significantly in HEK293 cells expressing *OATP-C*15* compared to those in cells expressing *OATP-C*1a*, the reference allele of *OATP-C*.[4] Based on these findings, we speculated that patients treated with pravastatin or atorvastatin who are carrying *OATP-C*15* have increased plasma concentrations of these drugs and are thus more susceptible to the myotoxic effects of these statins than are non-carrier patients treated with pravastatin or atorvastatin.

However, in our study two of seven patients who experienced myopathy after receiving pravastatin or atorvastatin did not possess *OATP-C*15* or mutated alleles of *OATP-C* that have been reported to decrease the function of OATP-C. Therefore, we sequenced all of the exons and exon-intron junctions of *OATP-C* for the DNA samples of these patients, and we found a novel nonsynonymous mutation of *OATP-C* located in exon 12 of this gene.

Materials and Methods

Human genomic DNA samples: DNA samples obtained from the two patients who experienced myopathy after receiving pravastatin or atorvastatin but did not possess *OATP-C*15* were used in the present study. None of the known mutant alleles of *OATP-C* that have

Received; October 15, 2004, Accepted; November 25, 2004

To whom correspondence should be addressed: Kan CHIBA, Ph.D., *Laboratory of Pharmacology and Toxicology, Graduate School of Pharmaceutical Sciences, Chiba University, 1-8-1 Inohana, Chuo-ku, Chiba 260-8675, Japan. Tel. & Fax. +81-43-226-2893, E-mail: kchiba@p.chiba-u.ac.jp*

Until October 11, 2004, the mutation described herein has not been registered in the NCBI dbSNP or JSNP database

Table 1. Primer sequences used for the analysis of *OATP-C*

Exon	Forward Primer (5′→3′)	Reverse Primer (5′→3′)	Note
2	CATTGACCTAGCAGAGTGGTAACG	GTGATCAATCCAAAACCAAAGAG	PCR and sequence
3	GAAATGATGCTTTATCAGTGTAGTGA	CCTGTGCAGTTATGACAACCAC	PCR and sequence
4	CATCTCCATTTTTCTTCATTCCA	GTACACACTTAGTGGGTATCTTC	PCR and sequence
	CATTGTCTTTGAGGGAAGGCACT		sequence
5	GTACTCTGGTAATTTGGGGAAGA	CTGTGTTGTTAATGGGCGAACT	PCR and sequence
	GTACTCTGGTAATTTGGGGAAGA		sequence
6–7	GGACTAATACACCATATTGTCAAAG	GCTGGATTTTATATTTATTCTGATT	PCR and sequence
6	TTGTAATAGAAATGCTAAAAT		sequence
7	TCCCTTTGTCTACTTTTGAA		sequence
8	CCTAGACAGTATCTGTTGCATTATGTCA	CTTCCACTTGTTATGTGCTCAAGA	PCR and sequence
9	TGTAAAGTACCCAGGATAACC	AGAGCAATAGTGACATCACAAGT	PCR and sequence
10	TTGATAGGTGCAGCAAACCAC	CAACCTATGTTGCTTCTCTTTAG	PCR and sequence
11	CTCTGCTTTCACTTTACTTC	CCTGATTGTGCCCTAAGCAGAC	PCR and sequence
12	GTCCAAAAGAGTATGTGCTCTGC	CAGCCTTGAGAGTTCATAGTA	PCR and sequence
	TGTATTTGCAGCACTGTTAGG		sequence

been reported to decrease its activity[5] were found in the DNA samples obtained from these patients. Written informed consent was obtained from the patients, and the study was approved by the Ethics Committee of the Graduate School of Pharmaceutical Sciences, Chiba University. We also studied fifty DNA samples obtained from healthy Japanese volunteers for the determination of allele frequency. Written informed consent was obtained from all of the volunteers, and the study was also approved by the Ethics Committee of the Graduate School of Pharmaceutical Sciences, Chiba University.

Polymerase chain reaction (PCR) conditions for sequencing: All exons and exon/intron boundaries of the *OATP-C* in the DNA samples obtained from the two patients were analyzed by PCR and direct sequencing. The primers used for amplification of the genomic DNA and direct sequencing are summarized in **Table 1.** DNA amplification was conducted in a reaction mixture (50 μL) containing 1–2 μg/mL genomic DNA, 1.2 mM $MgSO_4$, 5 mM dNTPs, 5 mM KOD buffer, 0.02 U/mL KOD-plus-polymerase and 0.2 μM of each primer. Thermocycling conditions consisted of initial denaturation for 3 minutes at 94°C followed by 35 cycles of denaturation at 96°C for 20 seconds, annealing at 57°C (reducing by 2°C every 3 cycles 2 times followed by 26 cycles at 51°C) for 30 seconds, and extension at 68°C for 25 seconds. Terminal elongation was performed at 68°C for 2 minutes. The PCR product was purified using Wizard® SV Gel and PCR Clean-Up System (Promega Corp., Madison, WI, USA) and directly sequenced on a CEQ™ 2000 DNA Analysis System (Beckman Coulter, Inc., Fullarton, CA, USA) with a CEQ™ DTCS Quick start kit (Beckman Coulter, Inc.). The reference sequence of *OATP-C* was obtained from GenBank (NT_000012.9).

DNA samples from healthy volunteers were analyzed by PCR and direct sequencing using the primers used for sequencing exon 12 (**Table 1**). PCR and thermocycling conditions were the same as the described above.

Results and Discussion

A novel nonsynonymous single nucleotide polymorphism (SNP) was found in one of the DNA samples from the two patients.

SNP: 041015OishiT001; GENENAME: *SLCO1B1*; ACCESSION NUMBER: NT_000012.9; LENGTH: 25 bases; 5′-CAATACAAGTCT T/G GAATTTATTTT-TC-3′. The SNP was 1628T>G in exon 12 of *OATP-C* (**Fig. 1**). In this SNP, Leu is substituted by Trp at position 543 in transmembrane-spanning domain 10 of OATP-C. Although the functional significance of this SNP is not known, it may cause functional impairment of OATP-C because it has been reported that nonsynonymous SNPs within the putative transmembrane domains in OATP-C result in severely reduced function of OATP-C due to its decreased plasma membrane expression.[5] This novel SNP was not found in any of the 50 DNA samples from healthy Japanese volunteers. The results suggest that the allele frequency of this novel variant allele of *OATP-C* is very low (<1%) in the Japanese population. However, OATP-C is responsible for the hepatocellular uptake of a broad range of endogenous and xenobiotic compounds, including bile acid, glucuronide and sulfate conjugates, methotrexate, pravastatin, rosuvastatin and cerivastatin.[6-9] Therefore, further studies are required to clarify the exact frequency in the Japanese population and the functional characteristics of this novel variant allele of *OATP-C*.

In conclusion, we found a novel nonsynonymous mutation (1628T>G) located in exon 12 of *OATP-C* in a DNA sample from a patient who experienced myopathy after receiving pravastatin. In this mutation, there is a substitution of Leu to Trp at position 543 in transmembrane-spanning domain 10 of OATP-C. The

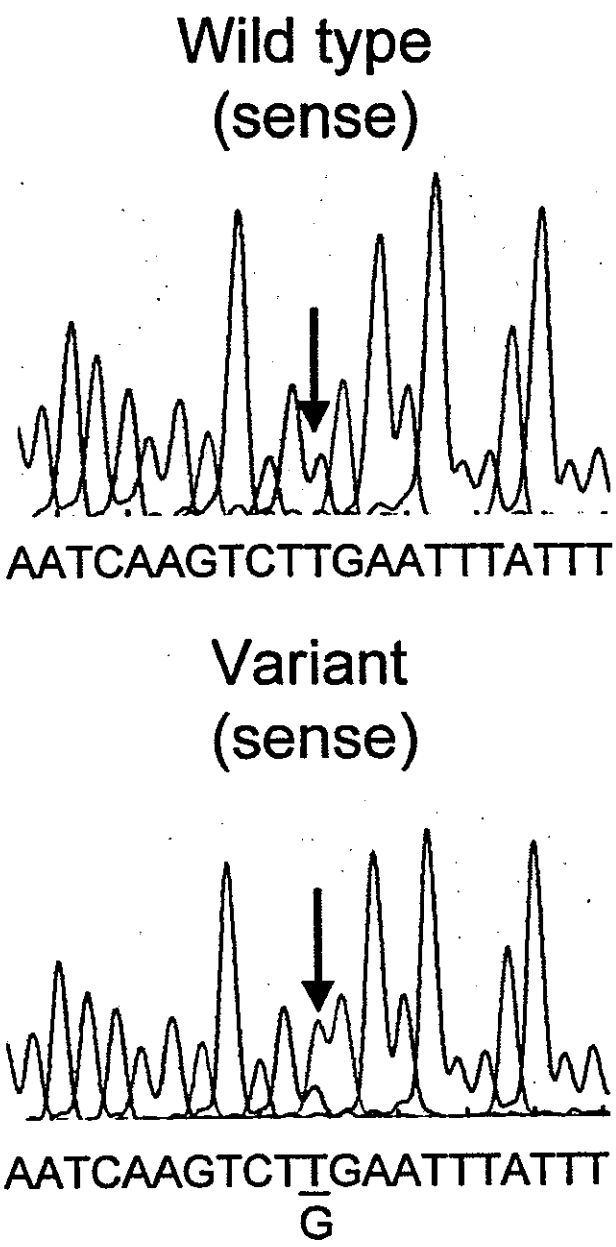

Fig. 1. Nucleotide sequences of *OATP-C* containing novel variant 041015OishiT001 (1628T>G) in exon 12. Arrows indicate the positions of the nucleotide change.

frequency of this mutation in the Japanese population appears to be very low (<1%).

Acknowledgements: This work was supported by grants-in-aid from the Ministry of Health, Labour and Welfare of Japan (Health and Labour Sciences Research Grants, Research on Human Genome, Tissue Engineering; Health and Labour Sciences Research Grants, Risk Analysis Research on Food and Pharmaceuticals), Tokyo, Japan.

References

1) Topol, E. J.: Intensive statin therapy—a sea change in cardiovascular prevention. *N. Engl. J. Med.*, 350: 1562-1564 (2004).
2) Thompson, P. D., Clarkson, P. and Karas, R. H.: Statin-associated myopathy. *Jama*, 289: 1681-1690 (2003).
3) Morimoto, K., Ueda, S., Seki, N., Igawa, Y., Kameyama, Y., Shimizu, A., Oishi, T., Hosokawa, M. and Chiba, K.: Candidate gene approach for the study of genetic factors involved in HMG-CoA reductase inhibitor-induced rhabdomyolysis. Eighteenth JSSX Annual Meeting, 8PE-32 (2003).
4) Kameyama, Y., Yamashita, K., Kobayashi, K., Hosokawa, M. and Chiba, K.: Functional characterization of *OATP-C* (*SLCO1B1*) variants, *OATP-C*5*, *OATP-C*15* and *OATP-C*15+C1007G*, by using transient expression systems of HeLa and HEK293 cells. Eighteenth JSSX Annual Meeting, 8PE-33 (2003).
5) Tirona, R. G., Leake, B. F., Merino, G. and Kim, R. B.: Polymorphisms in OATP-C: identification of multiple allelic variants associated with altered transport activity among European- and African-Americans. *J. Biol. Chem.*, 276: 35669-35675 (2001).
6) Shitara, Y., Itoh, T., Sato, H., Li, A. P. and Sugiyama, Y.: Inhibition of transporter-mediated hepatic uptake as a mechanism for drug-drug interaction between cerivastatin and cyclosporin A. *J. Pharmacol. Exp. Ther.*, 304: 610-616 (2003).
7) Abe, T., Kakyo, M., Tokui, T., Nakagomi, R., Nishio, T., Nakai, D. and *et al.*: Identification of a novel gene family encoding human liver-specific organic anion transporter LST-1. *J. Biol. Chem.*, 274: 17159-17163 (1999).
8) Nakai, D., Nakagomi, R., Furuta, Y., Tokui, T., Abe, T., Ikeda, T. and *et al.*: Human liver-specific organic anion transporter, LST-1, mediates uptake of pravastatin by human hepatocytes. *J. Pharmacol. Exp. Ther.*, 297: 861-867 (2001).
9) Simonson, S. G., Raza, A., Martin, P. D., Mitchell, P. D., Jarcho, J. A., Brown, C. D. and *et al.*: Rosuvastatin pharmacokinetics in heart transplant recipients administered an antirejection regimen including cyclosporine. *Clin, Pharmacol. Ther.*, 76: 167-177 (2004).

Pharmacogenetic roles of CYP2C19 and CYP2B6 in the metabolism of *R*- and *S*-mephobarbital in humans

Kaoru Kobayashi[a], Jun Morita[a], Kan Chiba[a], Atsuko Wanibuchi[b], Miyuki Kimura[b], Shin Irie[b], Akinori Urae[b], Takashi Ishizaki[c]

Objectives and methods **We assessed the relationship between the metabolism of *R*- and *S*-mephobarbital (MPB) and genetic polymorphisms of cytochrome P450 (CYP) 2C19 and CYP2B6. Nine homozygous extensive metabolizers (homo-EMs, *2C19*1/2C19*1*) of CYP2C19, ten heterozygous EMs (hetero-EMs, *2C19*1/2C19*2*, *2C19*1/2C19*3*) and eleven poor metabolizers (PMs, *2C19*2/2C19*2*, *2C19*3/2C19*3*, *2C19*2/2C19*3*) recruited from a Japanese population, received an oral 200 mg-dose of racemic MPB. Blood and urine samples were collected, and *R*-MPB, *S*-MPB and the metabolites, phenobarbital (PB) and 4′-hydroxy-MPB, were measured. Each subject was also genotyped for *CYP2B6* gene.**

Results **The mean area under the plasma concentration–time curve (AUC) of *R*-MPB was 92-fold greater in PMs than in homo-EMs. *R/S* ratios for AUC of MPB were much higher in PMs than in EMs (homo- and hetero-). The cumulative urinary excretion of 4′-hydroxy-MPB up to 24 h postdose was 21-fold less in PMs than in homo-EMs. The metabolic ratio of $AUC_{PB}/(AUC_{S\text{-}MPB} + AUC_{R\text{-}MPB})$ was higher in PMs than in EMs (homo- and hetero-). In addition, this metabolic ratio was lower in the carriers of *CYP2B6*6* compared with that in its non-carriers.**

Conclusions **Our results indicate that the 4′-hydroxylation of *R*-MPB is mediated via CYP2C19 and that the rapid 4′-hydroxylation of *R*-MPB results in a marked difference in the pharmacokinetic profiles between *R*-MPB and *S*-MPB in the different CYP2C19 genotypic individuals. In addition, a minor fraction of the interindividual variability in PB formation from MPB may be explainable by the *CYP2B6*6* allele. *Pharmacogenetics* 14:549–556 © 2004 Lippincott Williams & Wilkins**

Pharmacogenetics 2004, 14:549–556

Keywords: CYP2C19, CYP2B6, genetic polymorphism, mephobarbital, stereoselective metabolism

[a]Laboratory of Pharmacology and Toxicology, Graduate School of Pharmaceutical Sciences, Chiba University, Chiba, Japan, [b]Kyushu Pharmacology Research Clinic, Fukuoka, Japan and [c]Department of Pharmacology and Therapeutics, Graduate School of Medical and Pharmaceutical Sciences, Kumamoto University, Kumamoto, Japan.

Sponsorship: This work was supported by grants-in-aid from the Ministry of Health, Labour and Welfare of Japan (Health and Labour Sciences Research Grants, Research on Human Genome, Tissue Engineering; Health and Labour Sciences Research Grants, Risk Analysis Research on Food and Pharmaceuticals), Tokyo, Japan (to K.C.) and by a grant-in-aid (No. 99-2) from the Organization for Pharmaceutical Safety and Research (OPSR), Tokyo, Japan (to T.I.).

Correspondence: Takashi Ishizaki, MD, PhD, Department of Pharmacology and Therapeutics, Graduate School of Medical and Pharmaceutical Sciences, Kumamoto University, Oe-honmachi 5-1, Kumamoto 862-0973, Japan. Tel/fax: +81-96-371-4512; e-mail: kaoruk@p.chiba-u.ac.jp

Received 5 January 2004
Accepted 23 May 2004

Introduction

Mephobarbital (MPB, 5-ethyl-1-methyl-5-phenylbarbituric acid) is a chiral barbiturate which has been used as a racemate in the treatment of epilepsy since 1932. This drug undergoes an extensive hepatic metabolism in humans. Two routes of the metabolism have been described in humans [1–3]: aromatic hydroxylation to 4′-hydroxymephobarbital (OH-MPB) and *N*-demethylation to phenobarbital (PB). In addition, the *R*-enantiomer of MPB (*R*-MPB) is rapidly 4′-hydroxylated to yield OH-MPB, whereas *S*-enantiomer is principally *N*-demethylated to yield PB, the major metabolite in plasma [4,5]. As a result of this metabolic stereoselectivity, the oral clearance of *R*-MPB was much greater than that of *S*-MPB [5]. OH-MPB undergoes glucronidation and is mainly excreted in urine [3].

Küpfer and Branch [4] reported that the urinary recovery of OH-MPB after an oral administration of racemic MPB was not detected in the poor metabolizers (PMs) of *S*-mephenytoin and that OH-MPB in urine was not recovered in an extensive metabolizer (EM) administrated only *S*-MPB (90 mg), although it was recovered 33% in the EM administered the equal dose of *R*-MPB. In addition, our *in vitro* study demonstrated that the 4′-hydroxylation of MPB is preferential for *R*-enantiomer and its reaction is catalyzed by CYP2C19 [6]. These findings suggest that OH-MPB is exclusively formed from *R*-MPB by CYP2C19. However, the stereoselective disposition of MPB has only been studied in EMs, and no study in PMs of CYP2C19 has been conducted so far.

On the other hand, the *N*-demethylase activity of *S*-MPB appears to depend mainly on the catalytic capacity of CYP2B6 in human liver microsomes [7].

0960-314X © 2004 Lippincott Williams & Wilkins

DOI: 10.1097/01.fpc.0000114764.78957.22

CYP2B6 is involved in the biotransformation of many drugs including cyclophosphamide, which showed a substantial interindividual difference in the metabolism *in vitro* and *in vivo* [8,9]. A part of such interindividual variabilities can be caused by the genetic polymorphism of CYP2B6. Indeed, Lang *et al.* [10] have identified nine mutations of *CYP2B6* gene in a white population and termed the six different alleles as *CYP2B6*1* (wild-type), *CYP2B6*2*, *CYP2B6*3*, *CYP2B6*4*, *CYP2B6*5*, *CYP2B6*6* and *CYP2B6*7* by the haplotype analysis. Moreover, Lamba *et al.* [11] have reported the new additional alleles, *CYP2B6*8* and *CYP2B6*9*. However, very little has been reported on the effects of genetic polymorphism of CYP2B6 on the catalytic function *in vivo* or clinical implication [12].

The present study, therefore, was undertaken to investigate the stereoselective pharmacokinetic disposition and metabolism of MPB in the homo-EM, hetero-EM and PM groups of CYP2C19 recruited from a Japanese population. We also investigated the pharmacokinetic disposition of MPB in relation to the genetic polymorphism of CYP2B6.

Materials and methods

Drugs and chemicals

Racemic MPB was supplied by Mitsubishi Pharma Corp. (Osaka, Japan). OH-MPB was prepared from 4'-hydroxy-PB *via* *N*-methylation as described by Hiers and Hager [13].

Subjects

Thirty unrelated healthy Japanese male volunteers were enrolled in the current panel study. The subjects were interviewed and were judged as an identical Japanese ethnicity by lineage and birth. None had taken any drugs and beverages containing grapefruit for at least 1 week before the study. Each subject was physically normal and had no antecedent history of significant medical illness or hypersensitivity to any drugs. The study protocol was approved in advance by the ethics review board of Kyushu Pharmacology Research Clinic and by the ethics committee of Graduate School of Pharmaceutical Sciences, Chiba University. Each subject gave his written informed consent before the study.

Study protocol

Each volunteer received an oral 200-mg dose of racemic MPB (one tablet of Prominal, Winthrop Laboratories, Sydney, Australia) with 200 ml of water (around 8:00 am) after an overnight fast. Lunch and evening meals were provided at approximately 4 and 9 h after dosing, respectively. Serial venous blood samples (5 ml each) were collected at 0 (predose), 0.5, 1, 1.5, 2, 3, 4, 6, 8 and 12 h and 1, 2, 4, 8, 12 and 20 days after the dosing. Urine samples were collected at 0 to 24 h.

Analytical method

Concentrations of MPB enantiomers and PB in plasma were determined by a high pressure liquid chromatography (HPLC) method. Plasma (0.5 ml), 100 µl of 0.2 M K_2HPO_4 and 50 µl of secobarbital (as an internal standard) solution (10 µg/ml in methanol) were extracted with 5 ml of dichloromethane. The organic layer was evaporated and the residue was reconstituted with 200 µl of the mobile phase. Twenty µl of reconstituted filtrate by a 0.45 µm filter was injected onto the Jasco HPLC system (Tokyo, Japan) and a TSK-GEL ENANTIO OVM column (4.6 × 150 mm, Tosoh, Tokyo, Japan). The mobile phase consisted of potassium phosphate buffer (25 mM, pH 5.0)/ethanol in the proportion 100/7.5 v/v at a flow rate of 1.0 ml/min. The eluate was monitored at 215 nm.

The concentration of OH-MPB in urine was measured by HPLC after deconjugation. Urine (0.1 ml) was incubated at 37 °C for 2 h with 500 units of β-glucuronidase in 0.1 ml of potassium phosphate buffer (pH 5.0, 0.1 M). The deconjugated urine sample was extracted with 5 ml of dichloromethane after adding 50 µl of cyclobarbital (as an internal standard) solution (20 µg/ml in methanol) and 30 mg of NaCl. The organic layer was shaken with 2 ml of 0.5 N NaOH. The aqueous layer (1.5 ml) and 0.1 ml of 35% hydrochloride were extracted with 5 ml of dichloromethane. The residue of evaporated organic layer was reconstituted with 100 µl of the mobile phase, and 20 µl was directly injected onto the Hitachi HPLC system (Tokyo, Japan) and a CAPCELL PAK C_{18} UG120 column (4.6 × 250 mm, 5 µm; Shiseido, Tokyo, Japan). The mobile phase consisted of 50 mM potassium phosphate buffer (pH 5.0) and acetonitrile at a ratio of 75 : 25 (v/v) and a flow rate of 1 ml/min. The eluate was monitored at 215 nm.

Genotyping

The two *CYP2C19* mutants, *CYP2C19*2* and *CYP2C19*3* alleles, were genotyped by a polymerase chain reaction–restriction fragment length polymorphism (PCR–RFLP) method as described by Kubota *et al.* [14]. For *CYP2B6* mutants, *CYP2B6*2*, *CYP2B6*3*, *CYP2B6*4*, *CYP2B6*5*, *CYP2B6*6* and *CYP2B6*7* alleles were genotyped by using the PCR-RFLP method as described by Lang *et al.* [10], and the genotyping analysis was verified with a direct sequencing.

Pharmacokinetic and statistical analyses

Peak concentrations (C_{max}) and times to C_{max} (T_{max}) of *R*-MPB, *S*-MPB and PB were obtained directly from the plasma concentration–time data. The area under the plasma concentration–time curve (AUC) was calculated by the trapezoidal rule with extrapolation to the infinity. The elimination half-life ($t_{1/2}$) was calculated by linear regression analysis from the slope (k) of log-linear terminal concentration–time phases ($t_{1/2} = 0.693/$

k). The apparent oral clearance (CL/F) of *R*-MPB or *S*-MPB was estimated as follows: CL/F = dose/2/AUC/body weight, where dose represents that of racemic MPB (i.e. 200 mg). Urinary excretion of OH-MPB during the 0 to 24-h postdose period was calculated as the percentage molar amount of OH-MPB relative to the administered dose of racemic MPB.

All pharmacokinetic data are given as the mean ± standard deviation (SD). The statistical differences between the various group parameters were determined with either a paired Student's *t*-test or non-parametric Mann-Whitney *U*-test. A P value of <0.05 was considered as statistically significant.

Results

No clinically undesirable signs and symptoms possibly attributed to the administration of MPB were recognizable throughout the study period. All subjects completed the study according to the protocol.

Demographic and genotypic characteristics

The demographic and genotypic characteristics of the thirty normal healthy male volunteers enrolled in our study are summarized in Table 1.

Plasma concentration–time profiles of *R*-MPB, *S*-MPB and PB versus CYP2C19 genotypes

The mean (± SD) plasma concentration–time curves of *R*-MPB, *S*-MPB and its primary metabolite, PB, in the homo-EM (*2C19*1/2C19*1*), hetero-EM (*2C19*1/2C19*2, 2C19*1/2C19*3*) and PM (*2C19*2/2C19*2, 2C19*2/2C19*3, 2C19*3/2C19*3*) groups of CYP2C19 who took an oral 200-mg dose of racemic MPB are shown in Fig. 1(a, b and c, respectively). The mean plasma concentrations of *R*-MPB markedly differed among the three groups (Fig. 1a). In case of the EM status, *R*-MPB in plasma was undetectable throughout the total sampling time period in two homo-EMs and detectable at only one sampling time in two homo-EMs and a hetero-EM. Thus, the mean kinetic data on *R*-MPB (Table 2) could be estimated from the data

Table 1 Individual demographic characteristics and genotypic backgrounds of *CYP2C19* and *CYP2B6* of thirty male healthy subjects enrolled in the study

				Genotype	
Subject number	Age (yr)	Weight (kg)	Height (cm)	*CYP2C19*	*CYP2B6*
Group 1 (homo-EM for CYP2C19)					
2	21	54.1	166.9	*1/*1	*4/*6
3	21	51.7	171.3	*1/*1	*1/*1
7	28	62.3	175.8	*1/*1	*2/*6
9	22	62.6	172.2	*1/*1	*1/*6
19	22	59.6	174.0	*1/*1	*1/*6
20	21	70.5	172.1	*1/*1	*1/*1
23	20	64.6	169.1	*1/*1	*1/*1
27	21	54.9	167.3	*1/*1	*1/*1
29	23	66.1	168.6	*1/*1	*1/*1
Mean	22.1	60.7	170.8		
± SD	2.4	6.2	3.1		
Group 2 (hetero-EM for CYP2C19)					
1	20	69.3	172.7	*1/*2	*6/*6
5	20	54.3	161.7	*1/*2	*2/*6
6	23	53.6	168.2	*1/*2	*1/*1
10	33	69.5	176.8	*1/*2	*1/*6
11	20	74.7	175.1	*1/*2	*6/*6
12	21	58.7	173.7	*1/*2	*1/*6
18	22	71.1	178.4	*1/*3	*1/*1
22	23	60.5	165.4	*1/*2	*1/*1
26	25	54.7	168.3	*1/*2	*2/*6
28	23	72.3	181.7	*1/*2	*1/*1
Mean	23.0	63.9	172.2		
± SD	3.9	8.3	6.2		
Group 3 (PM for CYP2C19)					
4	31	79.9	182.8	*2/*2	*4/*6
8	30	59.9	172.3	*3/*3	*1/*6
13	23	54.4	170.6	*2/*3	*1/*1
14	28	59.2	180.1	*2/*2	*1/*1
15	21	71.4	175.5	*2/*3	*1/*1
16	21	50.0	158.8	*2/*3	*1/*2
17	40	61.2	169.7	*2/*2	*1/*1
21	21	66.6	181.7	*3/*3	*1/*4
24	20	57.4	168.0	*3/*3	*1/*1
25	23	67.1	173.3	*2/*2	*1/*2
30	24	75.0	175.3	*2/*2	*2/*4
Mean	25.6	63.8	173.5		
± SD	6.1	9.1	6.9		

Fig. 1

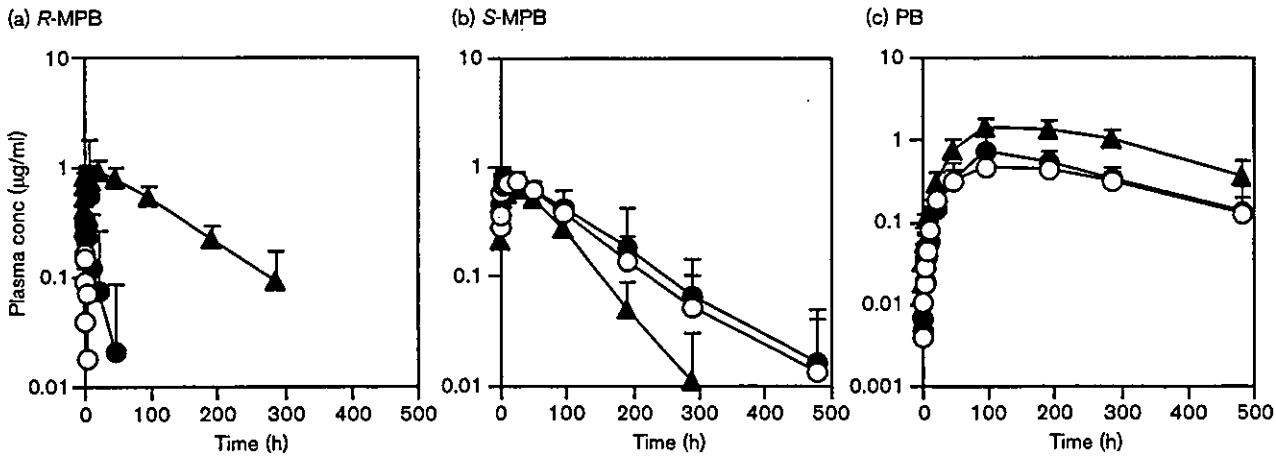

Plasma concentration–time profiles of *R*-mephobarbital (a), *S*-mephobarbital (b) and phenobarbital (c) after an oral 200-mg dose of racemic mephobarbital to the homo-EM ($n = 9$, open circles), hetero-EM ($n = 10$, closed circles) and PM groups of CYP2C19 ($n = 11$, closed triangles). Data are expressed as mean ± SD. MPB, mephobarbital; PB, phenobarbital.

Table 2 Pharmacokinetic parameters of *R*- and *S*-mephobarbital and phenobarbital obtained from the homo-EM, hetero-EM and PM groups of CYP2C19

Parameters	Homo EM ($n = 9$)	Hetero EM ($n = 10$)	PM ($n = 11$)
R-mephobarbital			
C_{max} (μg/ml)	0.3 ± 0.1	0.4 ± 0.3	1.0 ± 0.2***,†††
T_{max} (h)	1.3 ± 0.6	2.0 ±1.6	20.6 ± 13.0***,†††
AUC (μg/h/ml)	1.5 ± 0.3	6.6 ± 10.7	138.0 ± 37.5***,†††
$t_{1/2}$ (hr)	3.6 ± 1.5	6.8 ± 5.4	87.8 ± 19.9***,†††
CL/F (ml/h/kg)	1131.7 ± 286.7	730.2 ± 479.5*	12.2 ± 3.2***,††
S-mephobarbital			
C_{max} (μg/ml)	0.9 ± 0.2	0.8 ± 0.2	0.7 ± 0.2
T_{max} (h)	8.4 ± 9.1	10.6 ± 9.7	6.6 ± 8.7
AUC (μg/h/ml)	100.9 ± 20.0	113.7 ± 59.7	73.9 ± 36.2
$t_{1/2}$ (h)	76.4 ± 31.5	84.6 ± 37.1	68.7 ± 37.3
CL/F (ml/h/kg)	17.0 ± 3.7	16.0 ± 5.5	25.2 ± 9.8*,†
Phenobarbital			
C_{max} (μg/ml)	0.5 ± 0.2	0.7 ± 0.6	1.5 ± 0.4***,††
T_{max} (h)	128.0 ± 48.0	134.4 ± 49.6	139.6 ± 66.0
AUC (μg/h/ml)	184.4 ± 59.0	233.4 ± 164.2	519.2 ± 208.8***,††
$t_{1/2}$ (h)	184.0 ± 63.6	185.8 ± 93.2	143.3 ± 34.2

Data are expressed as means ± SD.
The mean kinetic data on *R*-mephobarbital are estimated from the data obtained from five homo-EMs and nine hetero-EMs.
*$P < 0.05$; and ***$P < 0.001$ versus homo-EM group.
†††$P < 0.001$; ††$P < 0.01$; and †$P < 0.05$ versus hetero-EM group.

obtained from the remaining five homo-EMs and nine hetero-EMs.

The mean plasma concentration–time curves of *S*-MPB (Fig. 1b) also indicated an intergenotypic difference in the CYP2C19 status. The mean plasma *S*-MPB concentrations at 96 to 288 h postdose were lower in the PM group than in the EM (homo- and hetero-) groups, implying that the elimination of *S*-MPB is considerably accelerated in the PM group. However, the mean plasma concentrations up to 48 h postdose revealed no differences among the three groups.

The plasma concentration–time profile of PB (Fig. 1c) showed a trend similar to that of *R*-MPB (Fig. 1a). There were the intergenotypic differences in the mean plasma PB concentrations between the PM and EM (homo- and hetero-) groups from 24 to 480 h postdose.

Pharmacokinetic analyses of *R*-MPB, *S*-MPB and PB versus CYP2C19 genotypes

The mean (± SD) pharmacokinetic data obtained from the three different genotypic groups are summarized in Table 2. There was a highly significant ($P < 0.001$) intergenotypic difference between the homo-EM and

PM groups in the mean kinetic parameters of *R*-MPB (Table 2). The mean C_{max}, T_{max}, AUC, $t_{1/2}$ and CL/F values were three-fold higher, 16-fold longer, 92-fold greater, 24-fold longer and 93-fold smaller, respectively, in the PM than in the homo-EM group. The mean kinetic values for PB showed similar differences between the PM and homo-EM groups as observed with *R*-MPB. The mean C_{max} and AUC values were significantly ($P < 0.001$) greater in the PM than in the homo-EM group. On the other hand, the mean kinetic data on *S*-MPB showed a behaviour opposite to those on *R*-MPB and PB. The mean AUC and $t_{1/2}$ were smaller and shorter, respectively, in the PM than in the homo-EM group, although the differences did not reach statistical significance. However, the mean CL/F value was significantly ($P < 0.05$) greater in the PM than in the homo-EM group.

Urinary excretion of OH-MPB versus CYP2C19 genotypes

The individual urinary excretion data of OH-MPB derived from the 0 to 24-h postdose period in the homo-EM, hetero-EM and PM groups are shown in Fig. 2. The mean (± SD) cumulative excretion at 24 h postdose was 10.9 ± 1.5% in homo-EMs, 9.5 ± 2.3% in hetero-EMs and 0.53 ± 0.31% in PMs. A subject (#12) with hetero-EM genotype (Table 1) showed a lower urinary excretion of OH-MPB (3.5% of dose) than the other subjects with the same hetero-EM genotype of CYP2C19 (8.4 to 11.7% of dose). PB was unmeasurable in urine samples of any of the subjects collected up to 24 h postdose.

Fig. 2

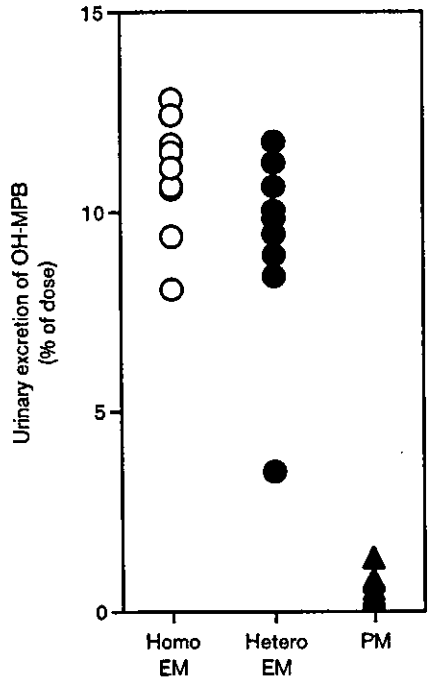

Individual data on urinary excretion of 4'-hydroxymephobarbital (% of dose) measured in 0 to 24 h after an oral 200-mg dose of racemic mephobarbital to the homo-EMs ($n = 9$, open circles), hetero-EMs ($n = 10$, closed circles) and PMs of CYP2C19 ($n = 11$, closed triangles). OH-MPB, 4'-hydroxymephobarbital.

R/S metabolic ratio for MPB

The mean (± SD) ratio of AUC for *R*-MPB to that for *S*-MPB (*R/S* metabolic ratio for AUC), was markedly greater in the PM than in the homo-EM group of CYP2C19 (2.069 ± 0.610 versus 0.014 ± 0.003). Subject 12, with the CYP2C19 hetero-EM genotype (Table 1) showed a greater *R/S* metabolic ratio for AUC than the ranging values observed in the other subjects with hetero-EM (0.543 versus 0.013–0.042). The mean *R/S* ratio for AUC in the hetero-EM group (0.023 ± 0.012), except for subject 12, was higher than that in the homo-EM and lower than that in the PM group.

CYP2B6 genotyping

Genotyping for six *CYP2B6* alleles was carried out in all 30 subjects recruited in this study (Table 1). The frequencies of *CYP2B6*2*, *CYP2B6*3*, *CYP2B6*4*, *CYP2B6*5*, *CYP2B6*6* and *CYP2B6*7* alleles were 10.0, 0, 6.7, 0, 23.3 and 0%, respectively. The present study showed a frequency pattern similar to the previous study performed in a Japanese population by Hiratsuka *et al.* [15].

PB formation index versus CYP2B6

To investigate the possible effect of *CYP2B6* alleles (*CYP2B6*2*, *CYP2B6*4* and *CYP2B6*6*) on the PB formation from MPB, the metabolic ratio (MR) of $AUC_{PB}/(AUC_{S\text{-MPB}} + AUC_{R\text{-MPB}})$ was calculated and used as a CYP2B6 metabolic activity index. As shown in Fig. 3a, the individuals carrying one or two *CYP2B6*6* alleles tended to have a lower MR in light of the MR in the individuals who are the *CYP2B6*6* non-carriers, although the differences among the 0, 1 and 2 *CYP2B6*6* carrier groups were not statistically significant. The mean MR of the individuals carrying one *CYP2B6*2* or one *CYP2B6*4* allele did not differ from that in all other subjects without carrying *CYP2B6*2* or *CYP2B6*4* allele.

The MR of $AUC_{PB}/(AUC_{S\text{-MPB}} + AUC_{R\text{-MPB}})$ was also compared among the three different *CYP2C19* genotype (homo-EM, hetero-EM and PM) groups. As shown in Fig. 3b, the mean MR in the PM group of CYP2C19 (2.5 ± 0.7) was significantly ($P < 0.05$) higher than that in the homo-EM (1.9 ± 0.7, by Mann–Whitney *U*-test) or hetero-EM group (1.9 ± 0.5, by Student's *t*-test).

Discussion

The present study indicated that the $t_{1/2}$ and AUC of *R*-MPB after an oral intake of racemic MPB was

Fig. 3

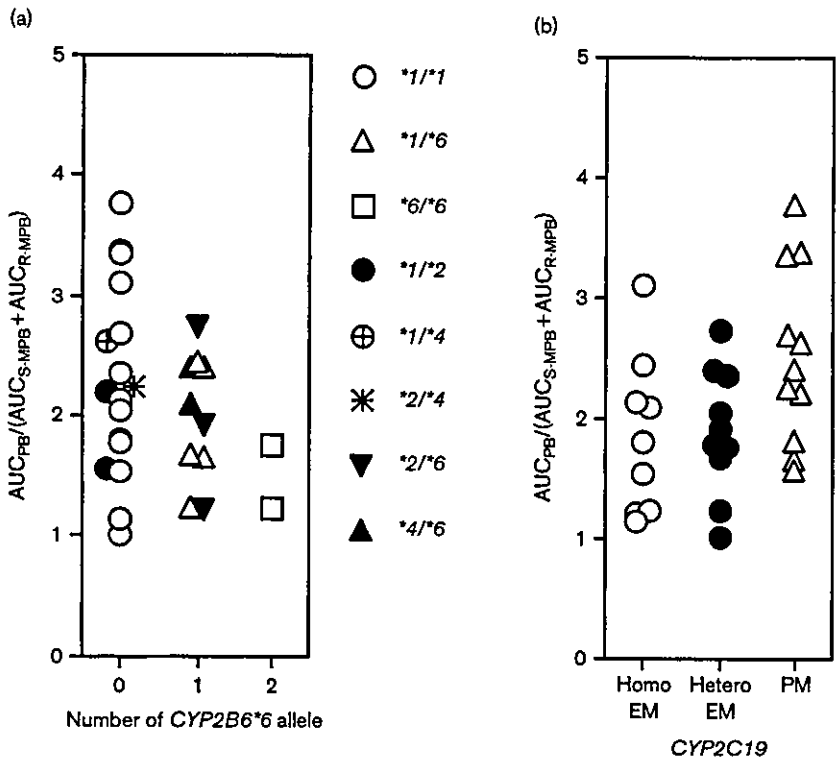

(a) Individual data on AUC ratio in carriers of two *CYP2B6*6* alleles ($n = 2$) and one *CYP2B6*6* allele ($n = 10$) and non-carriers of *CYP2B6*6* allele ($n = 18$). (b) Individual data on AUC ratio in homo-EMs ($n = 9$), hetero-EMs ($n = 10$) and PMs of CYP2C19 ($n = 11$). Area under the plasma concentration–time curve, AUC; AUC_{PB}, AUC for phenobarbital; $AUC_{S\text{-}MPB}$, AUC for *S*-mephobarbital; and $AUC_{R\text{-}MPB}$, AUC for *R*-mephobarbital.

markedly longer and greater (Fig. 1 and Table 2) in the PM group than in the (homo- and hetero-) EM groups of CYP2C19, respectively, and the urinary excretion of OH-MPB in the PM group of CYP2C19 was 21-fold lower than that in the EM groups (Fig. 2). Küpfer and Branch [4] reported that the urinary recovery of OH-MPB after the oral administration of racemic MPB was not detected in the PMs of CYP2C19, but that OH-MPB in urine was recovered in an EM administered *R*-MPB. In addition, our *in vitro* study demonstrated that the 4′-hydroxylation of MPB is preferential for *R*-enantiomer and its reaction is catalyzed by CYP2C19 [6]. Therefore, the findings obtained from the present *in vivo* study strongly indicate that the 4′-hydroxylation of *R*-MPB in humans *in vivo* is mainly catalyzed by CYP2C19 and this pathway of *R*-MPB is impaired in the PM individuals of CYP2C19.

On the other hand, the AUC of *S*-MPB in the PM group of CYP2C19 did not significantly differ from that in the EM groups of CYP2C19 (Table 2). The results obtained from the present *in vivo* study are consistent with the *in vitro* observation that *R*-MPB is 4′-hydroxylated by CYP2C19, but the metabolism of *S*-MPB is not catalyzed by CYP2C19 [6], in agreement with the *in vivo* observation that OH-MPB in urine was not recovered in an EM of CYP2C19 administrated only *S*-MPB [4]. Therefore, it is suggested that CYP2C19 is not responsible for the elimination of *S*-MPB from the human body.

As shown in Fig. 2, one data point derived from subject 12 (Table 1) deviated from the other data plots of the hetero-EMs, and, therefore, this hetero-EM individual was assumed to be an outlier in the group. The results suggested that subject 12, who was genotyped as *2C19*1/2C19*2* (Table 1), might have been a poor or low metabolizer of *R*-MPB, such as a PM of CYP2C19. To our knowledge, previous studies indicated that the two mutant alleles of *CYP2C19*, *CYP2C19*2* and *CYP2C19*3*, explain 100% of the PMs in the Japanese population [14]. To confirm the possibility that subject 12 may carry a novel mutant allele of *CYP2C19* in addition to *CYP2C19*2* allele, we sequenced all nine exons and exon–intron junctions of *CYP2C19* gene from the outlier and finally identified a novel SNP as *CYP2C19*16* [16].

One of the primary metabolites of MPB, PB, showed higher plasma levels in the PMs than in EMs of

CYP2C19 (Fig. 1 and Table 2). Our preliminary results from the *in vitro* experiments with human liver microsomes indicated that the formation of PB (i.e. via *N*-demethylation of MPB) occurred in a less stereoselective fashion and to a similar extent between the CYP2C19 EM- and PM-related liver microsomes (unpublished data), providing the following possibilities: (1) since *R*-MPB was extensively 4′-hydroxylated and rapidly eliminated in the EM individuals, PB should exclusively be formed from *S*-MPB; (2) in the PMs with the defective 4′-hydroxylation of *R*-MPB, *R*-MPB would be more available for the alternative route of metabolism by *N*-demethylation; and (3) if both *R*-MPB and *S*-MPB are presumed to contribute to the PB formation, plasma concentrations of PB should be higher in the PM than in the EM group. Nevertheless, no clinical signs and symptoms (e.g. sedation) possibly attributed to the administration of MPB were recognizable throughout the present study period in either of the EM or PM subjects of CYP2C19. This might occur because plasma concentrations of MPB and PB (i.e. <3 μg/ml) were much lower than therapeutic levels (i.e. for PB, 15 to 40 μg/ml is the therapeutic window). On the basis of the overall results obtained from the present study, we wish to propose a scheme of the assumptive metabolic pathways (i.e. via 4′-hydroxylation and *N*-demethylation) of MPB enantiomers and CYP isoforms involved in their pathways in EMs and PMs of CYP2C19 (Fig. 4).

Previously, Eadie *et al.* [17] reported that patients who were pretreated with PB showed a greater clearance of MPB (due probably to an induction by PB) and a rapid appearance of PB after administration of MPB than did the untreated patients. Since *S*-MPB is primarily metabolized to PB by CYP2B6 [7], pretreatment with PB

Fig. 4

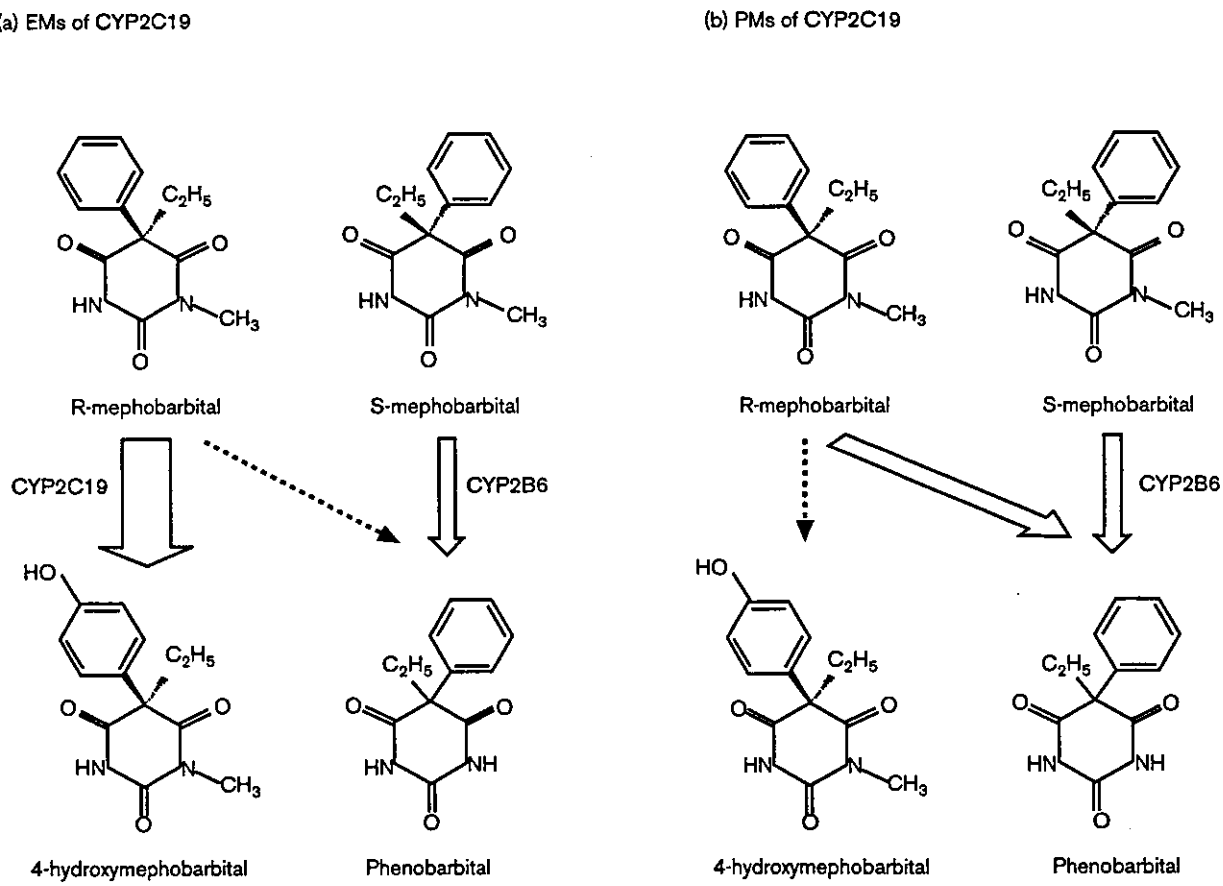

Proposed scheme of metabolic pathways of mephobarbital enantiomers and CYP isoforms involved in their pathways in EMs and PMs of CYP2C19. The thicknesses of open arrows indicate an assumptive degree of each of the two enzymes involved in the metabolic pathways of the two enantiomers of mephobarbital. The solid arrows with the dotted lines indicate a minor metabolic pathway of *R*-mephobarbital in the CYP2C19 EM and PM individuals. Whether *R*-mephobarbital would be metabolized to phenobarbital in humans and what CYP enzyme(s) would be involved in this pathway have remained unknown, although the authors have had their preliminary *in vitro* data with human liver microsomes, suggesting that *R*-mephobarbital is converted to phenobarbital (see Discussion).

would induce CYP2B6, thereby resulting in an accelerated elimination of *S*-MPB and production of PB. In this study, the PM group of CYP2C19 showed a slightly rapid elimination of *S*-MPB compared with the EM groups of CYP2C19 (Fig. 1b). In addition, the MR of $AUC_{PB}/(AUC_{S\text{-}MPB} + AUC_{R\text{-}MPB})$ was also higher in the PMs than in the EMs of CYP2C19 (Fig. 3b). These observations might have been due to an induction of CYP2B6 by PB, because the PM group of CYP2C19 had about three-fold higher plasma levels of PB than the EM groups (Fig. 1c).

Although the MR of $AUC_{PB}/(AUC_{S\text{-}MPB} + AUC_{R\text{-}MPB})$ was used for the metabolic index of MPB mediated via CYP2B6, no apparent outliers were observed (Fig. 3a). Among the six different *CYP2B6* alleles examined, only *CYP2B6*6* appeared to be associated with a moderately decreased MR, but due to the small sample size this difference did not reach statistical significance among the zero, one and two *CYP2B6*6* carriers. In the analysis of the *CYP2B6*6* allele in microsomes of human liver samples, a lower protein expression of CYP2B6.6, which was encoded by *CYP2B6*6*, has been reported [9,10]. On the other hand, V_{max} of recombinant CYP2B6.6 was higher than that of recombinant CYP2B6.1 [18,19]. Thus, the findings for the functional role of CYP2B6.6 obtained from the *in vitro* studies remain conflicting or inconclusive, but the lower protein expression would be compatible with our *in vivo* data. Since the subjects carrying *CYP2B6*2* or *CYP2B6*4* allele were rare and homozygotes of these alleles did not exist in our study subjects, further study is needed to assess whether *CYP2B6*2* and/or *CYP2B6*4* alleles would affect the MR. Moreover, Lamba *et al.* [11] have recently reported two new additional alleles of *CYP2B6* gene, *CYP2B6*8* and *CYP2B6*9*. Since *CYP2B6*6* (516G>T and 785A>G) overlapped with *CYP2B6*4* (785A>G) and *CYP2B6*9* (516G>T), it is not negated that some of our subjects genotyped as *2B6*1/2B6*6* in the present study might be carrying a genotype of *2B6*4/2B6*9*. However, *CYP2B6*9* has not yet been detected in Japanese population [15].

In conclusion, the present *in vivo* study strongly suggests that the 4′-hydroxylation of *R*-MPB is mediated via CYP2C19 in humans and that the stereoselective 4′-hydroxylation by this enzyme results in a marked difference in the pharmacokinetic profiles of *R*-MPB and *S*-MPB between the EM and PM individuals of CYP2C19. In addition, *CYP2B6*6* carriers tended to have a lower MR compared with that in other *CYP2B6*6* allele non-carriers, suggesting that a minor fraction of the interindividual variability in PB formation from MPB may be explainable by the absence or presence of *CYP2B6*6* allele.

Acknowledgement

We thank Dr Hooper (University of Queensland, Australia) for arrangement and gift of racemic mephobarbital (Prominal) tablets.

References

1 Kunze HE, Hooper WD, Eadie MJ. The metabolism of methylphenobarbitone in man. *Asean J Clin Sci* 1980; 1:115–119.
2 Hooper WD, Kunze HE, Eadie MJ. Pharmacokinetics and bioavailability of methylphenobarbital in man. *Ther Drug Monit* 1981; 3:39–44.
3 Hooper WD, Kunze HE, Eadie MJ. Qualitative and quantitative studies of methylphenobarbital metabolism in man. *Drug Metab Dispos* 1981; 9:381–385.
4 Küpfer A, Branch RA. Stereoselective mephobarbital hydroxylation cosegregates with mephenytoin hydroxylation. *Clin Pharmacol Ther* 1985; 38:414–418.
5 Lim WH, Hooper WD. Stereoselective metabolism and pharmacokinetics of racemic methylphenobarbital in humans. *Drug Metab Dispos* 1989; 17:212–217.
6 Kobayashi K, Kogo M, Tani M, Shimada N, Ishizaki T, Numazawa S, *et al.* Role of CYP2C19 in stereoselective hydroxylation of mephobarbital by human liver microsomes. *Drug Metab Dispos* 2001; 29:36–40.
7 Kobayashi K, Abe S, Nakajima M, Shimada N, Tani M, Chiba K, *et al.* Role of human CYP2B6 in *S*-mephobarbital *N*-demethylation. *Drug Metab Dispos* 1999; 27:1429–1433.
8 Boddy AV, Furtun Y, Sardas S, Sardas O, Idle JR. Individual variation in the activation and inactivation of metabolic pathways of cyclophosphamide. *J Natl Cancer Inst* 1992; 84:1744–1748.
9 Xie HJ, Yasar U, Lundgren S, Griskevicius L, Terelius Y, Hassan M, *et al.* Role of polymorphic human CYP2B6 in cyclophosphamide bioactivation. *Pharmacogenom J* 2003; 3:53–61.
10 Lang T, Klein K, Fischer J, Nussler AK, Neuhaus P, Hofmann U, *et al.* Extensive genetic polymorphism in human CYP2B6 gene with impact on expression and function in human liver. *Pharmacogenetics* 2001; 11:399–415.
11 Lamba V, Lamba J, Yasuda K, Strom S, Davila J, Hancock ML, *et al.* Hepatic CYP2B6 expression: gender and ethnic differences and relationship to *CYP2B6* genotype and CAR (constitutive androstane receptor) expression. *J Pharmacol Exp Ther* 2003; 307:906–922.
12 Kirchheiner J, Klein C, Meineke I, Sasse J, Zanger UM, Mürdter TE, *et al.* Bupropion and 4-OH-bupropion pharmacokinetics in relation to genetic polymorphisms in CYP2B6. *Pharmacogenetics* 2003; 13:619–626.
13 Hiers GS, Hager FD. Anisole. In: Gilman H ed. *Organic Syntheses 1*, 2nd edn, 1961. pp. 58–60. New York: John Wiley & Sons.
14 Kubota T, Chiba K, Ishizaki T. Genotyping of *S*-mephenytoin 4′-hydroxylation in an extended Japanese population. *Clin Pharmacol Ther* 1996; 60:661–666.
15 Hiratsuka M, Takekuma Y, Endo N, Narahara K, Hamdy SI, Kishikawa Y, *et al.* Allele and genotype frequencies of CYP2B6 and CYP3A5 in Japanese population. *Eur J Clin Pharmacol* 2002; 58:417–421.
16 Morita J, Kobayashi K, Wanibuchi A, Kimura M, Irie S, Ishizaki T, *et al.* A novel single nucleotide polymorphism (SNP) of the *CYP2C19* gene in a Japanese subject with lowered capacity of mephobarbital 4′-hydroxylation. *Drug Metabol Pharmacokin*, 2004; in press.
17 Eadie MJ, Bochner F, Hooper WD, Tyrer JH. Preliminary observations on the pharmacokinetics of methylphenobarbitone. *Clin Exp Neurol* 1978; 15:131–144.
18 Ariyoshi N, Miyazaki M, Toide K, Sawamura Y, Kamataki T. A single nucleotide polymorphism of CYP2B6 found in Japanese enhances catalytic activity by autoactivation. *Biochem Biophys Res Commun* 2001; 281:1256–1260.
19 Jinno H, Tanaka-Kagawa T, Ohno A, Makino Y, Matsushima E, Hanioka N, *et al.* Functional characterization of cytochrome P450 2B6 allelic variants. *Drug Metab Dispos* 2003; 31:398–403.

0090-9556/04/3201-7–9$20.00
DRUG METABOLISM AND DISPOSITION
DMD 32:7–9, 2004

Vol. 32, No. 1
1132/1111226
Printed in U.S.A.

Short Communication

CATALYTIC ROLES OF CYP2C9 AND ITS VARIANTS (CYP2C9*2 AND CYP2C9*3) IN LORNOXICAM 5′-HYDROXYLATION

(Received March 28, 2003; accepted September 4, 2003)

This article is available online at http://dmd.aspetjournals.org

ABSTRACT:

The effects of allelic variants of CYP2C9 (*CYP2C9*2* and *CYP2C9*3*) on lornoxicam 5′-hydroxylation were studied using the corresponding variant protein expressed in baculovirus-infected insect cells and human liver microsomes of known genotypes of CYP2C9. The results of the baculovirus expression system showed that CYP2C9.3 gives higher K_m and lower V_{max} values for lornoxicam 5′-hydroxylation than does CYP2C9.1. In contrast, K_m and V_{max} values of CYP2C9.1 and CYP2C9.2 for the reaction were comparable. Lornoxicam 5′-hydroxylation was also determined in liver microsomes of 12 humans genotyped for the *CYP2C9* gene (1/*1*, $n = 7$; **1/*2*, $n = 2$; **1/*3*, $n = 2$; **3/*3*, $n = 1$). A sample genotyped as **3/*3* exhibited 8- to 50-fold lower intrinsic clearance for lornoxicam 5′-hydroxylation than did samples genotyped as **1/*1*. However, the values for intrinsic clearance for **1/*3* were within the range of values exhibited by samples of **1/*1*. In addition, no appreciable differences were observed in kinetic parameters for lornoxicam 5′-hydroxylation between **1/*1* and **1/*2*. In conclusion, this study showed that lornoxicam 5′-hydroxylation via CYP2C9 was markedly decreased by the substitution of Ile359Leu (CYP2C9.3), whereas the effect of the substitution of Arg144Cys (CYP2C9.2) was nonexistent or negligible. Additional in vivo studies are required to confirm that individuals with homologous *CYP2C9*3* allele exhibit impaired lornoxicam clearance.**

Lornoxicam (also known as chlortenoxicam) [6-chloro-4-hydroxy-2-methyl-*n*-2-pyridyl-5*H*-thieno(2,3-*e*)-[1,2]-thiazine-2-carboxamide-1,1-dioxide] is a nonsteroidal anti-inflammatory drug that decreases prostaglandin synthesis by inhibiting cyclooxygenase (Radhofer-Welte and Rabasseda, 2000). Exhibiting analgesic, antipyretic, and anti-inflammatory effects, lornoxicam has been clinically available in certain European countries since 1995. Since no unchanged form is detectable in excreted material, lornoxicam appears to be eliminated predominantly by hepatic biotransformation. The enzyme responsible for the main metabolic pathway, 5′-hydroxylation of lornoxicam, is cytochrome P450 2C9 (CYP2C9) (Bonnabry et al., 1996).

CYP2C9 is the principal enzyme responsible for the metabolism of numerous clinically important drugs, such as amitriptyline, fluoxetine, losartan, phenytoin, *S*-warfarin, tolbutamide, and many nonsteroidal antirheumatics, including oxicams (Miners and Birkett, 1998). To date, more than 10 allelic variants have been described for the *CYP2C9* gene (Goldstein, 2002). Among them, *CYP2C9*2* (Arg144Cys), *CYP2C9*3* (Ile359Leu), *CYP2C9*5* (Asp360Glu), and *CYP2C9*6* (frame shift by the deletion of an adenine at the 818 cDNA base pair) have been reported to affect the metabolism and clinical toxicity of drugs in vitro and in vivo (Dickmann et al., 2001; Kidd et al., 2001). However, the degree of reduction of activity and changes in kinetic parameters appear to be highly substrate-dependent (Takanashi et al., 2000). In addition, a few studies have been performed regarding whether heterozygotes of the *CYP2C9* alleles exhibit lower metabolic activity than homozygotes of the *CYP2C9*1* allele (Bhasker et al., 1997; Yamazaki et al., 1998; Hermida et al., 2002; Lee et al., 2002).

Address correspondence to: Izumi Iida, Department of Drug Metabolism, Research Center, Taisho Pharmaceutical Co., Ltd., 403, Yoshino-cho 1-chome, Saitama-shi, Saitama 330-8530, Japan. E-mail: Izumi.Iida@po.rd.taisho.co.jp

In the present study, we examined the effects of allelic variants of CYP2C9 on lornoxicam 5′-hydroxylation by comparing the kinetic parameters of lornoxicam 5′-hydroxylation with CYP2C9.1, CYP2C9.2, or CYP2C9.3, which are the CYP2C9 proteins corresponding to *CYP2C9*1*, *CYP2C9*2*, or *CYP2C9*3* alleles, expressed in baculovirus-infected insect cells and liver microsomes of 12 white people genotyped for the *CYP2C9* gene.

Materials and Methods

Chemicals. Lornoxicam was synthesized at Taisho Pharmaceutical Co., Ltd. (Saitama, Japan). 5′-Hydroxylornoxicam was supplied by Nycomed (Roskilde, Denmark). Piroxicam was purchased from ICN Biomedicals Inc. (Costa Mesa, CA). Other chemicals and reagents used in this study were of the highest quality commercially available.

Enzyme Preparations. Microsomes from baculovirus-infected insect cells expressing CYP2C9.1, CYP2C9.2, and CYP2C9.3 (catalog numbers, P218, P209, and P242) were obtained from BD Gentest (Woburn, MA). These were coexpressed with NADPH-P450[1] oxidoreductase. The P450 contents in recombinant CYP2C9.1, CYP2C9.2, and CYP2C9.3 were 667, 426, and 741 pmol P450/mg protein, whereas the values for the cytochrome *c* reductase activity were 980, 590, and 800 nmol/min/mg protein, respectively. Individual human liver microsomes (HG3, HG23, HG30, HG42, HG43, HG56, HG66, HG70, HG89, HG93, HG112, and HK27) were also purchased from BD Gentest. The genotyping of the liver samples used in this study was carried out for the detection of *CYP2C9*2* and *CYP2C9*3* by BD Gentest. Table 1 lists the donor genotypes for the *CYP2C9* gene.

Lornoxicam 5′-Hydroxylase Activity. Lornoxicam 5′-hydroxylase activities in human liver microsomes or microsomes from the expression system were determined by HPLC. The standard incubation conditions were chosen based on the results of preliminary experiments varying both incubation times and concentrations of microsomal proteins. A typical incubation mixture (0.2 ml of the total volume) contained 100 mM Tris buffer (pH 7.4), an NADPH-

[1] Abbreviations used are: used are: P450, cytochrome P450; HPLC, high performance liquid chromatography.

TABLE 1

Kinetic parameters for 5'-hydroxylornoxicam formation from lornoxicam in cDNA-expressed CYP2C9 recombinant systems and human liver microsomes

	K_m	V_{max}	V_{max}/K_m
	μM	*pmol/min/pmol total P450*	*μl/min/pmol total P450*
cDNA-expressed CYP2C9 recombinant systems			
CYP2C9.1	0.83 ± 0.15[a]	0.406 ± 0.016	0.489 ± 0.065
CYP2C9.2	0.91 ± 0.08	0.495 ± 0.010[b]	0.544 ± 0.041
CYP2C9.3	1.95 ± 0.09[b]	0.097 ± 0.001[b]	0.050 ± 0.002[b]
Human liver microsomes			
HG23 **1/*1*	0.79	0.256	0.324
HG30 **1/*1*	0.81	0.278	0.343
HG42 **1/*1*	1.28	0.069	0.054
HG66 **1/*1*	0.76	0.142	0.187
HG70 **1/*1*	0.77	0.189	0.245
HG89 **1/*1*	0.66	0.168	0.255
HG112 **1/*1*	1.08	0.182	0.169
HG43 **1/*2*	0.83	0.106	0.128
HG56 **1/*2*	0.81	0.115	0.142
HG3 **1/*3*	0.72	0.143	0.199
HG93 **1/*3*	1.72	0.145	0.084
HK27 **3/*3*	2.82	0.019	0.007

[a] Kinetic parameters expressed as mean ± SD (n = 3).
[b] $p < 0.05$ vs. CYP2C9.1.

generating system (1 mM $NADP^+$, 8 mM glucose 6-phosphate, 5 mM $MgCl_2$, 2 IU/ml glucose-6-phosphate dehydrogenase), lornoxicam, and 0.25 mg/ml microsomal protein of human livers. The reaction was initiated by the addition of the microsomes after 5-min preincubation at 37°C. The reaction mixtures were incubated for 20 min, and reactions were terminated by the addition of 0.1 ml of acetonitrile, including 3 μM piroxicam as an internal standard. After removal of the protein by centrifugation at 10,000 rpm for 5 min, a 10-μl portion of the supernatant was subjected to HPLC. For recombinant P450s, the incubation mixture was of the same composition as mentioned above, except that 25, 25, or 200 pmol P450/ml, respectively, were used for microsomes from baculovirus-infected insect cells expressing CYP2C9.1, CYP2C9.2, or CYP2C9.3. For kinetic determinations, lornoxicam concentrations ranging from 0.5 to 125 μM were used.

HPLC analyses were performed according to the method of Suwa et al. (1993), with slight modifications. The HPLC system consisted of a 2690 separation module Alliance system equipped with a Millennium32 chromatointegrator and a 2487 dual λUV-visible spectrophotomonitor (Waters, Tokyo, Japan). Chromatography was performed on an XTerra RP18 column (50 × 2.1 mm; particle size = 3.5 μm; Waters) eluted at 0.2 ml/min with the following mobile phase: 14.5% acetonitrile, 50 mM KH_2PO_4. The eluent was monitored at 380 nm. The column temperature was 60°C.

Statistical Analysis. All experiments were performed in triplicate, and the mean values for each data point were used for analysis. Enzyme kinetic parameters (K_m, V_{max}) were estimated by curve-fitting metabolite formation rate data by the single-enzyme Michaelis-Menten equation and Eadie-Hofstee plot. All graphical analyses were performed by nonlinear regression using SAS Version 6.1 (SAS Institute, Cary, NC). Differences in kinetic parameters among different *CYP2C9* genotypes were evaluated for statistical significance by Dunnett's multiple comparison.

Results and Discussion

Figure 1A shows the formation of 5'-hydroxylornoxicam by recombinant systems prepared from the cell line expressing the variants of CYP2C9. Simple Michaelis-Menten kinetics were noted for lornoxicam metabolism in all samples studied. The kinetic parameters of lornoxicam 5'-hydroxylation for CYP2C9.1, CYP2C9.2, and CYP2C9.3 are shown in Table 1. CYP2C9.3 (Leu359) had higher K_m values and lower V_{max} than did CYP2C9.1 (wild-type, Ile359) for lornoxicam 5'-hydroxylation. The differences in K_m and V_{max} values between CYP2C9.1 and CYP2C9.3 were about 2- and 4-fold, respectively.

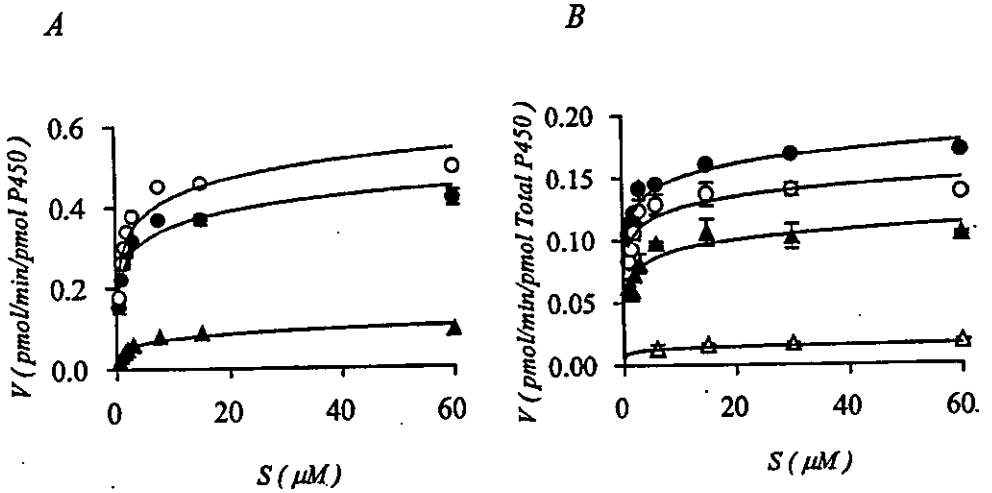

FIG. 1. *Michaelis-Menten plots for 5'-hydroxylation of lornoxicam by cDNA-expressed CYP2C9.1 (●), CYP2C9.2 (○), and CYP2C9.3 (▲) (A), and representative Michaelis-Menten plots for 5'-hydroxylation of lornoxicam by human liver microsomes from four genotyped livers (B).*

In A, results are expressed as mean ± S.D. of triplicate experiments. In B, liver microsomes of HG89 (●, genotyped as **1/*1*), HG3 (▲, genotyped as **1/*2*), HG43 (○, genotyped as **1/*3*), and HK27 (△, genotyped as **3/*3*) were used for the plots.

In terms of intrinsic clearance (V_{max}/K_m, the intrinsic capacity of an enzyme to metabolize a substrate), the values for CYP2C9.3 showed 10-fold smaller V_{max}/K_m values for the reaction than did CYP2C9.1. This finding is in good agreement with a previous report of Takanashi et al. (2000) in which CYP2C9.3 expressed in yeast cells exhibited lower intrinsic clearance than did CYP2C9.1 for oxidation of other oxicams, such as tenoxicam 5′-hydroxylation and piroxicam 5′-hydroxylation. These results suggest that the amino acid substitution of Ile359 for Leu359 also affects the metabolic capacity of CYP2C9 in addition to the affinity of CYP2C9 for lornoxicam. The effect of this change on both the K_m and V_{max} values may be explained by the proposal that CYP2C9 amino acid 359 lies within putative substrate recognition sequence 5 in the CYP2 family (Lewis, 2002).

In contrast, K_m, V_{max}, and intrinsic clearance (V_{max}/K_m) of lornoxicam 5′-hydroxylation for CYP2C9.1 (wild-type, Arg144) and CYP2C9.2 (Cys144) expressed in baculovirus-infected insect cells were comparable (Table 1). There was no significant difference between CYP2C9.1 and CYP2C9.2 in V_{max}/K_m values for the reaction. This finding is consistent with previous reports that CYP2C9.2 has catalytic functions similar to those of CYP2C9.1 for the oxidation of tolbutamide, *S*-warfarin, and torsemide (Sullivan-Klose et al., 1996; Miners et al., 2000). However, Rettie et al. (1994) reported that the V_{max} values of the CYP2C9.2 for *S*-warfarin 7-hydroxylation were lower than that of CYP2C9.1. Crespi and Miller (1997) showed that the magnitude of the difference in V_{max} for *S*-warfarin between CYP2C9.1 and CYP2C9.2 depends on the expression system used, and is influenced by the ratio of NADPH-P450 oxidoreductase to P450. Thus, it is necessary to use human liver samples genotyped as **2/*2* to clarify the effect of the substitution of Arg144Cys for CYP2C9 on the activity in human liver microsomes.

We determined the kinetic parameters of lornoxicam 5′-hydroxylation from liver microsomes derived from 12 human samples genotyped for the *CYP2C9* gene. The formation of 5′-hydroxylornoxicam by human liver microsomes showed simple Michaelis-Menten kinetic behavior (Fig. 1B). Using Eadie-Hofstee plots, we confirmed that a single kinetic parameter could be determined in the reaction. As shown in Table 1, apparent K_m values for lornoxicam 5′-hydroxylation ranged from 0.76 to 1.28 μM in microsomes of livers genotyped as **1/*1*. The K_m values for liver microsomes of samples genotyped as **1/*2* or **1/*3* ranged from 0.72 to 1.72 μM. Only a microsome sample genotyped as **3/*3* exhibited a high K_m value (2.82 μM). The sample genotyped as **3/*3* exhibited a lower V_{max} value (0.019 pmol/min/pmol total P450) than the other samples genotyped as **1/*1*, **1/*2*, or **1/*3* (0.069–0.278 pmol/min/pmol total P450). Thus, samples genotyped as **3/*3* showed 8- to 50-fold lower intrinsic clearance (V_{max}/K_m, 0.007 μl/min/pmol total P450) than samples genotyped as **1/*1* and other heterozygous alleles of *CYP2C9* (0.054–0.343 μl/min/pmol total P450), although only one sample was genotyped as **3/*3*. The substitution of Ile359Leu for CYP2C9 also appears to decrease the intrinsic clearance of lornoxicam 5′-hydroxylation in human liver microsomes. In addition, the present study using human liver microsomes containing samples genotyped as **1/*2* or **1/*3* showed that the heterozygous alleles of *CYP2C9*2* or *CYP2C9*3* did not always have lower intrinsic clearance for lornoxicam 5′-hydroxylation than **1/*1*.

Rare cases of subjects with higher than expected plasma concentrations after the administration of lornoxicam have been reported (Turner and Johnston, 1990; Ravic et al., 1991). Since 5′-hydroxylation is the main metabolic pathway of lornoxicam in humans, it has been speculated that the increase in plasma concentrations is attributable to defective metabolism of lornoxicam. Our results indicate that it may be possible that certain subjects, exhibiting high area under the curve and C_{max} values associated with delayed elimination, are the poor-metabolizer phenotypes of CYP2C9, although their actual genotypes were unknown.

In conclusion, the present study showed that the lornoxicam 5′-hydroxylation via CYP2C9 was markedly reduced by the substitution of Ile359 for Leu359 (CYP2C9.3), whereas the effect of the substitution of Arg144 for Cys144 (CYP2C9.2) was nonexistent or negligible. Additional in vivo studies are required to confirm that individuals with the homologous *CYP2C9*3* allele exhibit impaired lornoxicam clearance.

Research Center, Taisho Pharmaceutical Co., Ltd., Saitama, Japan (I.I., A.M., M.Ar. M.H., M.Ak., S.H.); and Laboratory of Pharmacology and Toxicology, Graduate School of Pharmaceutical Sciences, Chiba University, Chiba, Japan (K.K., K.C.)

IZUMI IIDA
ATSUNORI MIYATA
MASAYUKI ARAI
MITSUYO HIROTA
MASAYUKI AKIMOTO
SHOHEI HIGUCHI
KAORU KOBAYASHI
KAN CHIBA

References

Bhasker CR, Miners JO, Coulter S, and Birkett DJ (1997) Allelic and functional variability of cytochrome P4502C9. *Pharmacogenetics* 7:51–58.

Bonnabry P, Leemann T, and Dayer P (1996) Role of human liver microsomal CYP2C9 in the biotransformation of lornoxicam. *Eur J Clin Pharmacol* 49:305–308.

Crespi CL and Miller VP (1997) The R144C change in the *CYP2C9*2* allele alters interaction of the cytochrome P450 with NADPH:cytochrome P450 oxidoreductase. *Pharmacogenetics* 7:203–210.

Dickmann LJ, Rettie AE, Kneller MB, Kim RB, Wood AJ, Stein CM, Wilkinson GR, and Schwarz UI (2001) Identification and functional characterization of a new CYP2C9 variant (CYP2C9*5) expressed among African Americans. *Mol Pharmacol* 60:382–387.

Goldstein JA (2002) Polymorphisms in the human CYP2C subfamily. *Drug Metab Rev* 34 (Suppl 1):5.

Hermida J, Zarza J, Alberca I, Montes R, Lopez ML, Molina E, and Rocha E (2002) Differential effects of 2C9*3 and 2C9*2 variants of cytochrome P-450 CYP2C9 on sensitivity to acenocoumarol. *Blood* 99:4237–4239.

Kidd RS, Curry TB, Gallagher S, Edeki T, Blaisdell J, and Goldstein JA (2001) Identification of a null allele of CYP2C9 in an African-American exhibiting toxicity to phenytoin. *Pharmacogenetics* 11:803–808.

Lee CR, Pieper JA, Hinderliter AL, Blaisdell JA, and Goldstein JA (2002) Evaluation of cytochrome P4502C9 metabolic activity with tolbutamide in *CYP2C9*1* heterozygotes. *Clin Pharmacol Ther* 72:562–571.

Lewis DFV (2002) Homology modeling of human CYP2 family enzymes based on the CYP2C5 crystal structure. *Xenobiotica* 32:305–323.

Miners JO and Birkett DJ (1998) Cytochrome P4502C9: an enzyme of major importance in human drug metabolism. *Br J Clin Pharmacol* 45:525–538.

Miners JO, Coulter S, Birkett DJ, and Goldstein JA (2000) Torsemide metabolism by CYP2C9 variants and other human CYP2C subfamily enzymes. *Pharmacogenetics* 10:267–270.

Radhofer-Welte S and Rabasseda X (2000) Lornoxicam, a new potent NSAID with an improved tolerability profile. *Drugs Today* 36:55–76.

Ravic M, Johnston A, Turner P, Takacs F, and Rosenow DE (1991) The effect of repeated oral doses of lornoxicam on antipyrine elimination in normal human volunteers. *Hum Exp Toxicol* 10:375–377.

Rettie AE, Wienkers LC, Gonzalez FJ, Trager WF, and Korzekwa KR (1994) Impaired (S)-warfarin metabolism catalysed by the R144C allelic variant of CYP2C9. *Pharmacogenetics* 4:39–42.

Sullivan-Klose TH, Ghanayem BI, Bell DA, Zhang Z-Y, Kaminsky LS, Shenfield GM, Miners JO, Birkett DJ, and Goldstein JA (1996) The role of the CYP2C9-Leu359 allelic variant in the tolbutamide polymorphism. *Pharmacogenetics* 6:341–349.

Suwa T, Urano H, Shinohara Y, and Kokatsu J (1993) Simultaneous high-performance liquid chromatographic determination of lornoxicam and its 5′-hydroxy metabolite in human plasma using electrochemical detection. *J Chromatgr* 617:105–110.

Takanashi K, Tainaka H, Kobayashi K, Yasumori T, Hosokawa M, and Chiba K (2000) CYP2C9 Ile^{359} and Leu^{359} variants: enzyme kinetic study with seven substrates. *Pharmacogenetics* 10:95–104.

Turner P and Johnston A (1990) Clinical pharmacokinetic studies with lornoxicam. *Postgrad Med J* 66:s28–s29.

Yamazaki H, Inoue K, and Shimada T (1998) Role of two allelic variants (Arg144Cys and Ile359Leu) of cytochrome P4502C9 in the oxidation of tolbutamide and warfarin by human liver microsomes. *Xenobiotica* 28:103–115.

総説

薬物トランスポーターの遺伝的多型と臨床的意義

家入一郎[1)]/大坪健司[2)]

〔SUMMARY〕 薬物の吸収，分布，排泄を規定する薬物トランスポーターが数多くクローニングされ，その発現部位，輸送方向性，基質薬物が明らかとされつつある．同時に遺伝子多型によるヒト生体中での機能評価ならびに個人差の解明が急ピッチで進んでいる．その結果，薬物トランスポーターは相互作用などを含む薬物療法全般に重要な役割を果たすことが指摘されるに至っている．薬物代謝酵素に加え薬物トランスポーターの遺伝子多型情報は個別適正化使用―オーダーメイド医療―を一歩前進させる情報と期待される．〔臨床検査　48：139-147，2004〕

〔KEYWORDS〕 薬物輸送蛋白，薬物トランスポーター，遺伝的多型，機能変化

はじめに

薬物の体内動態や効果に見る大きな個人差の原因が関与する蛋白をコードする遺伝子の多型から説明されつつある．その代表は，薬物代謝酵素であるが，代謝を受けるためには肝臓に薬物が運ばれる，すなわち分布する必要がある．近年，この分布のみならず，吸収や排泄過程に関与する薬物輸送蛋白(薬物トランスポーター)が数多く同定され，その機能が明らかにされるとともに，代謝酵素と同様にその機能の差が遺伝子多型から予測されようとしている．薬物トランスポーターの生体機能を考える場合には，その基質薬物，発現部位，輸送方向性が重要となる．本稿では，現在までに日本人を中心に詳細な遺伝子多型解析が行われ，その機能への関与が明らかとなった薬物トランスポーターを取り上げ，遺伝子多型診断に基づいた医薬品適正使用の一端を紹介する．

主な薬物トランスポーターの種類

薬物トランスポーターは，肝，腎，小腸などの消化管，脳，肺といった様々な組織の上皮細胞(あるいは血管内皮細胞)に発現し，薬物の生体膜輸送(取り込みや汲み出し)に重要な役割を果たしている．表1には，現在までにヒトで確認されている主な薬物トランスポーターをまとめた．薬物トランスポーターは，ABCトランスポーター(ATP binding cassette)と溶質トランスポーター(solute carrier superfamily；SLC)の2つに大別される．前者は，ATPの加水分解エネルギーを駆動力とし，細胞内から細胞外へ薬物を排出する．P-糖蛋白(P-gp，遺伝子名が*MDR1*)やMRP1，MRP2(別名cMOAT)などが代表的であり，癌細胞に見られる抗癌剤の多剤耐性の原因蛋白としてよく知られている．有機イオントランスポータースーパーファミリー(SLC22A)は有機アニオントランスポーター(OAT)，有機カチオントランスポーター(OCT)，カルニチントランスポーター(OCTN)の3種類のファミリーで構成されており，主に低脂肪性イオン薬物の細胞内への取り込み過程に関与する．一方，脂溶性の比較的高いアニオン性薬物の取り込みには，OATファミリーとは構造的にも異なるOATPファミリ

1）IEIRI Ichiro　鳥取大学医学部附属病院薬剤部・助教授・副薬剤部長
2）OTSUBO Kenji　同・教授・薬剤部長

表1　ヒトに見られる主な薬物トランスポーター

family/subfamily	gene	symbol	発現臓器	基質となる医薬品
ABC B subfamily	*MDR1*	*ABCB1*	肝臓，腎臓，小腸，脳，胎盤など	ジゴキシン，ベラパミル，シクロスポリン，サキナビル，ロペラミド，エトポシド，ドキソルビシン，オンダンセトロン，キニジンなど
	MDR3 (MDR2)	*ABCB4*	肝臓	
	BSEP	*ABCB11*	肝臓	
ABC C subfamily	*MRP1*	*ABCC1*	肝臓，脳	メトトレキセート，葉酸
	MRP2 (cMOAT)	*ABCC2*	肝臓，腎臓，小腸	メトトレキセート，葉酸，プラバスタチン，テモカプリラート，CPT-11
	MRP3	*ABCC3*	肝臓，腎臓，小腸	
	MRP4	*ABCC4*	腎臓	
ABC G subfamily	*BCRP*	*ABCG2*	肝臓，脳，胎盤	4-メチルウンベリフェロン(主に硫酸抱合体)
OATP family	*OATP-B*	*SLC21A9*	肝臓，小腸，腎臓	
	OATP-C (OATP2, LST-1)	*SLC21A6*	肝臓	プラバスタチン，リファンピシン，チロキシン
	OATP8	*SLC21A8*	肝臓	
OCT family	*OCT1*	*SLC22A1*	肝臓	ドパミン，メトフォルミン
	OCT2	*SLC22A2*	腎臓	ドパミン
	OCT3	*SLC22A3*	肝臓以外の諸臓器	
OCTN family	*OCTN1*	*SLC22A4*	広範囲な臓器	L-カルニチン，キニジン，ベラパミル
	OCTN2	*SLC22A5*	広範囲な臓器	L-カルニチン
OAT family	*OAT1*	*SLC22A6*	腎臓	非ステロイド性抗炎症薬，プロスタグランディンE2，βラクタム抗生物質
	OAT2	*SLC22A7*	肝臓，腎臓	サリチル酸，アセチルサリチル酸
	OAT3	*SLC22A8*	腎臓	プラバスタチン，シメチジン
Peptide transporter PEPT	*PEPT1*	*SLC15A1*	肝臓，腎臓，小腸	ジペプチド，トリペプチド，βラクタム抗生物質，ACE阻害薬，ベスタチン，バラシクロビル
	PEPT2	*SLC15A2*	腎臓	

ー(SLC21A)が関与する．小腸や腎臓に発現するペプチドトランスポーター(PEPT, SLC15A)は，その名のとおり，蛋白質の消化産物であるジペプチドやトリペプチドといった小分子ペプチドをH^+濃度勾配を駆動力として細胞内に取り込む．PEPTには，PEPT1とPEPT2の2種類の分子種が単離されており，発現部位や基質への親和性が異なる．

薬物トランスポーターの基本的な機能

例として肝臓と腸管に発現する数種類の薬物トランスポーターを取り上げ，その機能を概説する．

1. 肝臓

冒頭にも触れたように，肝臓で薬物が代謝されるためには，最初に肝細胞の膜を透過して細胞内へ取り込まれる必要がある．肝細胞の類洞側膜には図1に示すように，多くのトランスポーターが発現しており，薬物はこれらのトランスポーターにより細胞内に取り込まれる．取り込まれた薬物は細胞内で代謝酵素により，第1相(酸化反応)あるいは第2相(抱合反応)の代謝を受けて，水溶性の高い化合物に変換される．こうして代謝された薬物は，胆管側膜に発現する排出型のトランスポーターにより胆汁中へ排泄される．高脂血症治療薬として繁用されるHMG-CoA還元酵素阻害剤

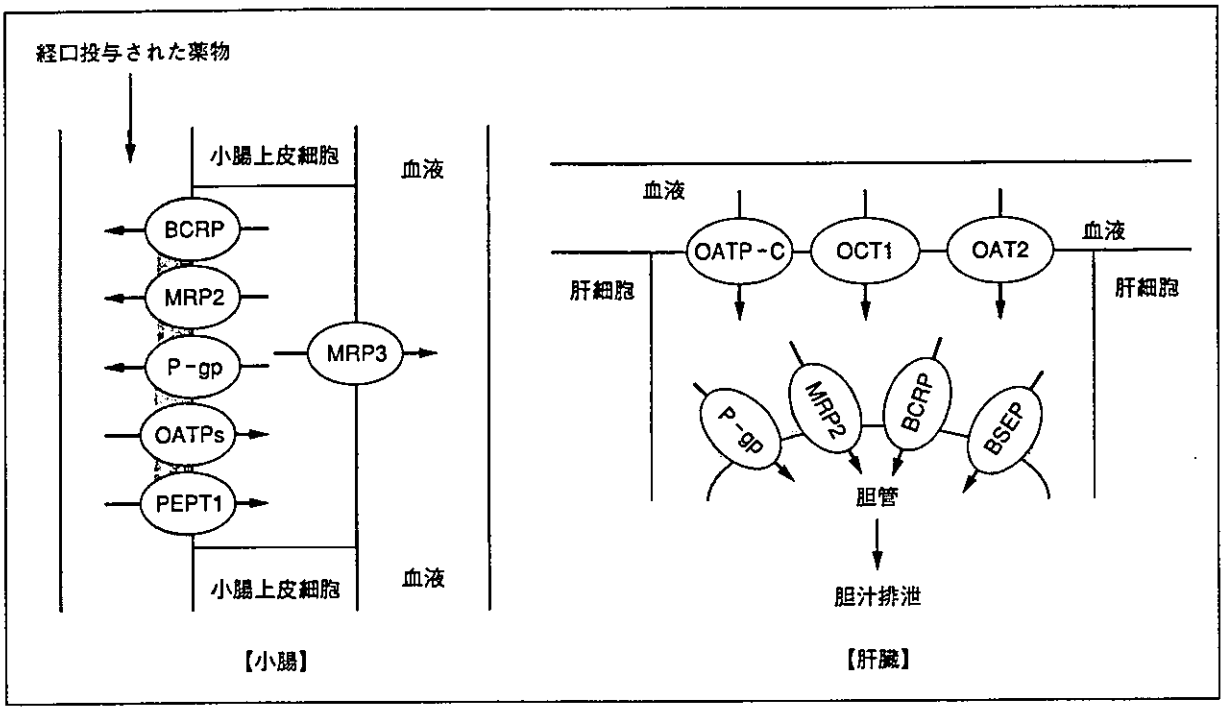

図1　小腸と肝臓での薬物トランスポーターの発現部位と輸送方向性

であるプラバスタチンは，肝に特異的に発現するOATP-Cにより選択的に肝細胞に取り込まれ，作用の後，MRP2により胆汁排泄される．これ以外に，代謝された薬物が類洞側膜に発現するトランスポーターにより再度，血液中に排出される経路も存在する．このように，トランスポーターを介した薬物輸送は，代謝過程の一環と考えられ第3相の代謝反応とも呼ばれる．

2．腸管

経口投与された薬物は，小腸の上皮細胞に取り込まれた後，血液中に到達する．この一連の過程が吸収と呼ばれ，取り込みと血液中への汲み出しにトランスポーターが関与する(図1)．ここでは，*MDR1*遺伝子の産物であるP-gpを取り上げる．P-gpは小腸上皮細胞の管腔側(腸管側)に発現しており，別のトランスポーターにより細胞内に取り込まれた薬物を再度，腸管側に排出する．すなわち，薬物が吸収されるのを妨げる働きをする．また，P-gpは，脳毛細血管内皮細胞にも発現しており，血液から脳実質に薬物が到達するのを防ぐ．このように，P-gpの生体中での機能は，薬物を含む異物から生体を守る働きをしているといえる．癌細胞が抗癌剤を細胞外に排出する耐性と同じ働きといえる．

薬物トランスポーター遺伝子多型

現在までに数多くの遺伝子について多型が報告されている．表2に一部をまとめた．変異の多くは一塩基置換(SNPs)であり，代謝酵素に見られる遺伝子の全欠損や重複などの報告はない．また，変異のヒトでの機能評価中に注目された現象として，ハプロタイプがある．すなわち，いくつかのSNPsが連鎖不平衡にあるもので，*MDR1*[1]や*OATP-C*[2]で詳細な検討が行われている．さらに，薬物代謝酵素と同様に，変異の頻度には人種間で差がみられることから，以下に述べる薬物の体内動態や効果には人種差の存在が示唆される．

遺伝子多型の臨床的意義

1．体内動態や効果への関与

薬物トランスポーター遺伝子の多型解析は疾患との関連が中心であったが，薬物の体内動態や効果についての知見がここ2,3年で急速に蓄積されつつある．機能評価は，ノックアウトマウスや発現細胞実験が中心であるが，ここでは，ヒトでの

表2　主な薬物トランスポーター遺伝子の多型と日本人での頻度

gene	mutation	effect	frequecy(%)
MDR1	−129 T>C	—	8.3(C allele)
	1236 T>C	—	35.4(C allele)
	2677 G>T	893 Ala>Ser	41.7(T allele)
	2677 G>A	893 Ale>Thr	21.8(A allele)
	2956 A>G	986 Met>Val	0.5(G allele)
	3435 C>T	—	49.0(T allele)
MRP1	128 G>C	43 Cys>Ser	1.0(C allele)
	218 C>T	73 Thr>Ile	1.0(T allele)
	2168 G>A	723 Arg>Gln	7.3(A allele)
	3173 G>A	1058 Arg>Gln	1.0(A allele)
MRP2	−24 C>T	—	18.8(T allele)
	1249 G>A	417 Val>Ile	12.5(A allele)
	2302 C>T	768 Arg>Trp	1.0(T allele)
	2366 C>T	789 Ser>Phe	1.0(T allele)
	4348 G>A	1450 Ala>Thr	1.0(A allele)
BCRP	34 G>A	12 Val>Met	18.0(A allele)
	376 C>T	126 Gln>Stop codon	1.0(T allele)
	1515 C>delete	509 Met>Stop codon	0.5(deletion)
OATP-B	109 C>T	37 Pro>Thr	30.9(T allele)
	935 G>A	312 Arg>Gln	32.8(A allele)
	1457 C>T	486 Ser>Phe	30.9(T allele)
OATP-C	388 A>G	130 Asn>Asp	62.9(G allele)
	521 T>C	174 Val>Ala	15.8(C allele)
	1454 G>T	485 Cys>Phe	0.8(T allele)
OAT3	1166 C>T	389 Ala>Val	0.8(T allele)
OCT1	123625 C>T	341 Phe>Leu	16.1(T allele)
	126827 A>G	408 Met>Val	82.8(G allele)

表中の変異は，われわれの研究室で検討を加えたもので，一部のみを抜粋した．また，健常成人から得たゲノムDNAを試料とした．

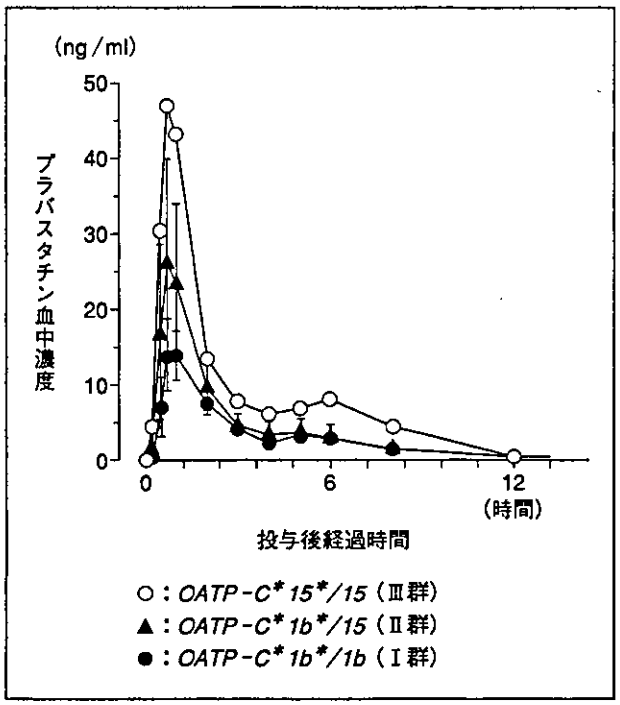

図2　*OATP-C* 遺伝子型とプラバスタチン血中濃度推移

機能を中心に述べる．

1）*OATP-C* 遺伝子

OATP-Cは肝の類洞側膜に発現し，薬物の肝への取り込み(uptake)に働く．現在までに17種類のハプロタイプが報告されている[2]．その中で，アミノ酸の置換を伴う130 Asn>Aspと174 Val>Alaが注目される．130 D/D 174 V/V(I群，130位と174位がそれぞれAsp，Valのホモ接合体で，*OATP-C*1b/*1b* の遺伝子型)，130 D/D 174 V/A(II群，174位のみがヘテロ接合体で，*OATP-C*1b/*15* 型)，130 D/D 174 A/A(III群，174位がAlaのホモ接合体で，*OATP-C*15/*15* 型)の3群にOATP-Cの基質薬物であるプラバスタチンを単回投与した際の血中濃度の推移を図2に示す[3]．II群，III群，すなわち，174位に変異を有する被検者では，全身クリアランスの低下と血中濃度の上昇が認められている．

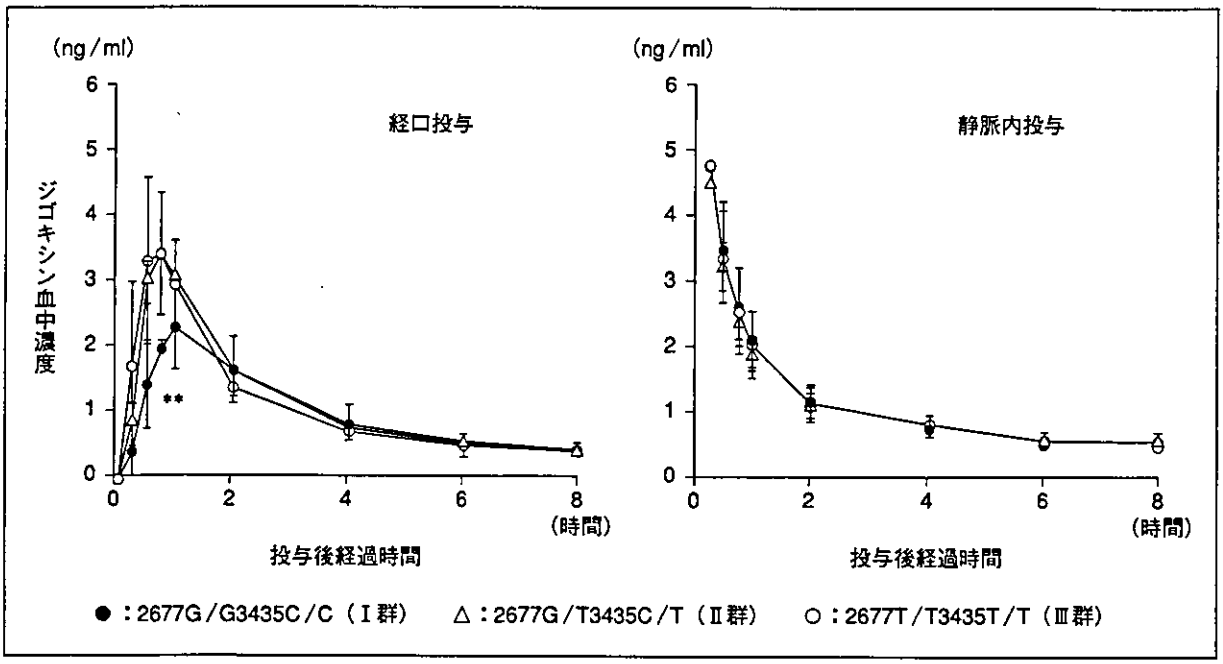

図3 *MDR1* 遺伝子型とジゴキシン血中濃度推移

ホモ型変異保有者(III群)の全身クリアランスはI群の50%程度であり，かつ，ヘテロ型変異保有者(II群)には，両ホモ型保有者の中間値を示すgene-dose effectが観察されている．*OATP-C*遺伝子多型のヒトでの機能評価は現在のところ，本研究のみであるが，発現系による *in vitro* 研究がいくつか報告されている．それらの報告では174位の変異により基質薬物の輸送能の低下が見られる[2]．したがって，ヒトで観察された変異保有者での血中濃度の上昇(全身クリアランスの低下)は，プラバスタチンの肝への取り込みの低下が原因と考えられる．プラバスタチンなどのHMG-CoA還元酵素阻害剤は肝に取り込まれることでコレステロール低下作用を示すことから，本変異保有者では，期待する効果が得られないことが予想される．この仮説は今後の検討を通して明らかにされるべき課題である．

2）*MDR1* 遺伝子

表2に示すように，*MDR1*遺伝子には数多くの変異が報告されているが，翻訳領域に存在する変異では，exon 21の2677G>T/Aとexon 26の3435C>Tが注目されている[4,5]．当初，3435C>Tの機能変化が報告されたが[5]，本変異はアミノ酸の置換を伴わないことから，別の変異との関連が示唆されていた．その後の研究により，両変異は連鎖不平衡にあり，高率で同時に生じることが明らかとなった[4]．図3には，われわれが行った心不全の治療薬であるジゴキシンでの検討結果を示した[6]．検討は2677G/G3435C/C(I群)，2677G/T3435C/T(II群)，2677T/T3435T/T(III群)の遺伝子型を有する健常成人にジゴキシンを経口と静注で投与し，吸収率を算出することで行った．興味あることに，ジゴキシンを静脈内投与した際の血中濃度には3群間で差は見られなかったが，経口投与時には，変異がない群(I群)で低い濃度推移が観察された．さらに，吸収率もIII群>II群>I群の順で低くなり，I群とIII群の差は約20%であった．この検討では2つの結果がポイントである．1つ目は，I群で吸収率が低かった点である．先にも述べたように，腸管に発現するP-gpは上皮細胞に到達した薬物を腸管側へ再度汲み出すことから，吸収率を下げる働きをする．したがって，本検討の結果からは，変異は機能低下，すなわち，腸管への排出能の低下の原因となり，その結果，吸収率の増加＝血中濃度の上昇につながったと考えられる．2つ目は，多型の関与が経口投与時にのみ見られた点である．静脈内投与したジゴキシンは腸管上皮細胞に発現するP-gpと直接，接触することがない．したがって，P-gpの影響を受けることが少ない．この結果は，投与する剤形により体内動態に違いが生じることを示し，臨床的にも極めて重要な現象であ

表3　*MDR1* 遺伝子多型のヒトでの機能評価

遺伝子変異	基質薬物	対象	機能変化
3435C>T	ジゴキシン	健常成人	T/T>C/C(最高血中濃度)
2677G>T 3435C>T	ジゴキシン	健常成人	M/M>W/M>W/W(吸収率) W/W>W/M>M/M(腎・分泌クリアランス)
3435C>T	ジゴキシン	健常成人	C/C>T allele 保有者(血中濃度)
3435C>T	フェニトイン	健常成人	T/T>C/C(血中濃度)
3435C>T	シクロスポリン	健常成人	(T/T+T/C)>(C/C)(血中濃度)
3435C>T	シクロスポリン	腎移植患者	変化なし(血中濃度や拒絶反応の頻度)
3435C>T	ノルトリプチリン	鬱患者	T/T>C/T>C/C(薬剤性低血圧)
3435C>T	ネルフィナビル エファビレンツ	HIV-1 患者	T/T>C/T>C/C(CD 4 細胞数や回復率) C/C>C/T>T/T(最低血中濃度)
2677G>T 3435C>T	ステロイド	小児心移植患者	W/W>W/M>M/M(ステロイド服用期間)
2677G>T/A	タクロリムス	部分肝移植患者	(T/A)>G(中枢性副作用頻度)

W：野生型アレル，M：変異アレル，　〔文献 7) より一部抜粋〕

る．さらに，この現象は，次に述べる相互作用とも関連があり，P-gp の基質で経口と注射の両方の剤形がある医薬品を使用する際には注意が必要と言える．

薬物トランスポーター遺伝子多型の機能評価は，*MDR1* 遺伝子が最もよく検討が加えられており，情報も多い．一部を表3にまとめた[7]．効果との関連では，三環系抗うつ薬ノルトリプチリンによる薬剤性低血圧(3435T/T で生じやすい)[8]，HIV-1 治療薬による CD 4 細胞数や免疫機能改善効果(3435T/T で高い)[9]，心移植小児患者におけるステロイド使用期間(2677T/T3435T/T で短い)[10] などがあり，いずれも変異による機能低下を支持する結果である．一方，体内動態への関与を見ると，必ずしも一致した知見が得られている訳ではない．ジゴキシンを用いたわれわれの検討では，変異保有者(2677T/T3435T/T)で高い血中濃度推移が得られたが，3435C/C で高いとする逆の知見の報告もある[11]．アレルギー治療薬であるフェキソフェナジンでも同様な結果が得られている[12,13]．論文間で異なった知見が得られる原因として，以下が考えられる．(a)指標とする変異が報告間で異なる：*MDR1* 遺伝子の詳細な構造が明らかとなり，ハプロタイプによる対象の選択が望まれる．(b)基質特異性：ジゴキシンやフェキソフェナジンは，P-gp の基質薬物であると同時にそれぞれ，OATP8 と OATP-A の基質であることが知られている[14,15]．一般的に薬物トランスポーターの基質認識性は広く，多様な構造の薬物を輸送するものが多い．さらに，上述した *OATP-C* 以外の分子種である *OATP-B* や *OATP8* にも遺伝子多型がある．これらのヒトでの機能変化については不明であるが，体内動態への関与は否定できない．

3) *MRP2* (*cMOAT*) 遺伝子

MRP2 も P-gp と同様に抗癌剤などの多剤耐性に関与する(細胞内から細胞外へ各種抗癌剤の排出を行う)．肝臓の胆管側膜に強発現する MRP2 は，肝臓内で産生される各種抱合体を基質としており，抱合型ビリルビンの肝細胞から胆汁への排泄も担当する．抱合型ビリルビン高値を主徴とする先天性疾患である Dubin-Johnson 症候群は MRP2 の排泄障害により生じ，原因となる遺伝子変異が多く同定されている[16]．しかし，*MRP2* 遺伝子上に存在するすべての変異が原因となる訳ではなく，日本人で比較的頻度の高い 417Val>Ile の関与はないと考えられる(著者未発表データ)．

4) その他の遺伝子

OAT3 は，近位尿細管上皮細胞の側低膜側に発現し，基質薬物の血液からの取り込みに関与する．この過程は尿細管分泌の第一段階であることから，薬物の尿排泄を考える場合重要といえる．基質薬物であるプラバスタチンの尿細管分泌クリアランスへの多型の関与を検討した結果，723T>A，389Ala>Val の影響は見られなかっ